Interplay of order and disorder in two-dimensional critical systems with mixed boundary conditions

E. Eisenriegler
Institute for Advanced Simulation, Theoretische Physik der lebenden Materie (IAS-2), Forschungszentrum Jülich, D-52425 Jülich, Germany

(Received 4 October 2025; accepted 13 January 2026; published 4 February 2026)

In spin systems such as the Ising model, the local order and disorder can be characterized by the order-parameter and energy density profiles $\langle\sigma(\mathbf{r}_1)\rangle$ and $\langle\epsilon(\mathbf{r}_2)\rangle$, respectively. Does increasing the order at $\mathbf{r}_1$ always decrease the disorder at $\mathbf{r}_2$? Does increasing the disorder at $\mathbf{r}_2$ always decrease the order at $\mathbf{r}_1$? The answer to these questions is contained in the cumulant response function $\langle\sigma(\mathbf{r}_1)\epsilon(\mathbf{r}_2)\rangle^{(\mathrm{cum})}$. This correlation function vanishes in the unbounded bulk but not in systems with fixed-spin boundary conditions. Using the universal operator-product expansion of $\sigma(\mathbf{r}_1)\epsilon(\mathbf{r}_2)$ and exact results for the Ising model, we analyze $\langle\sigma(\mathbf{r}_1)\epsilon(\mathbf{r}_2)\rangle^{(\mathrm{cum})}$ in two-dimensional critical systems defined on the $x-y$ plane with mixed $+$ and $-$ boundary conditions. Particularly interesting behavior is found when either of the operators σ or ϵ is located on a "zero line" in the $x-y$ plane, along which $\langle\sigma(\mathbf{r})\rangle$ vanishes. Results for half-plane, triangular, and rectangular geometries are presented.

DOI: 10.1103/14gm-31hg

I. INTRODUCTION

Order and disorder are basic concepts in the field of phase transitions and critical phenomena. Interesting effects arise in critical systems with boundaries [1,2]. Here we investigate the interplay of order and disorder in the two-dimensional Ising model with mixed boundary conditions [3–6] right at its bulk-critical point. In Ising systems the local order and disorder can be characterized by the averages of the density operators $\sigma(\mathbf{r})$ and $\epsilon(\mathbf{r})$ of the order parameter and the energy which are odd and even, respectively, under the change of direction of all Ising spins. In the conformal classification [7], $\sigma(\mathbf{r})$ and $\epsilon(\mathbf{r})$ are the only primary operators of the two-dimensional Ising model.

For a given configuration of Ising spins, $\sigma(\mathbf{r})$ is, in the sense of coarse graining [8], proportional to the difference of the number of up spins and down spins in a volume element around $\mathbf{r}$, while $-\epsilon(\mathbf{r})$ is proportional to the sum of the products of nearest neighbor spins in the volume element with its bulk average subtracted [9]. Thus $\langle\sigma(\mathbf{r})\rangle$ specifies the direction and magnitude of the local spin alignment and provides a measure of the local order. The quantity $\langle\epsilon(\mathbf{r})\rangle$ vanishes in the bulk and increases as the correlation between neighboring spins decreases and thus characterizes the local disorder [10].

It is convenient to normalize the two operators via their two-point function in the bulk or, equivalently, via the leading term in their operator product expansion "OPE" [5,7] such that

$$\sigma(\mathbf{r}_1)\sigma(\mathbf{r}_2) \to \frac{1}{|\mathbf{r}_{12}|^{1/4}} + \cdots,$$
$$\epsilon(\mathbf{r}_1)\epsilon(\mathbf{r}_2) \to \frac{1}{|\mathbf{r}_{12}|^{2}} + \cdots. \tag{1.1}$$

Here $\mathbf{r}_{12} \equiv \mathbf{r}_1 - \mathbf{r}_2 \equiv -\mathbf{r}_{21}$.

Our goal is to investigate the response $\delta\langle\epsilon(\mathbf{r}_2)\rangle$ of the disorder $\langle\epsilon\rangle$ at point $\mathbf{r}_2$ to a weak up ordering imposed at point $\mathbf{r}_1$. This is given by the response function

$$\langle\sigma(\mathbf{r}_1)\epsilon(\mathbf{r}_2)\rangle^{(\mathrm{cum})} \equiv \langle\sigma(\mathbf{r}_1)\epsilon(\mathbf{r}_2)\rangle - \langle\sigma(\mathbf{r}_1)\rangle\langle\epsilon(\mathbf{r}_2)\rangle. \tag{1.2}$$

This same function also describes the response $\delta\langle\sigma(\mathbf{r}_1)\rangle$ of $\langle\sigma\rangle$ at point $\mathbf{r}_1$ to a weak increase of disorder imposed at point $\mathbf{r}_2$.

The response function (1.2) vanishes in the unbounded bulk, due to the $\sigma \to -\sigma$ symmetry. In systems with boundary spins fixed in the up or down direction, this symmetry is broken and the response function is nonvanishing.

Before analyzing the response function (1.2) in detail, we consider some *intuitive* expectations. As for the geometry, a useful example is the upper half plane bounded by the x axis.

(i) For a uniform $+$ boundary, $\langle\sigma\rangle$ is positive everywhere in the upper half plane. Increasing the up-ordering, e.g., by applying a local magnetic field at $\mathbf{r}_1$, also tends to further align spins in the surroundings in the up direction. Thus both $\delta\langle\epsilon(\mathbf{r}_2)\rangle$ and the response function (1.2) are negative. The same conclusion follows from increasing the disorder at $\mathbf{r}_2$, e.g., by local heating, which reduces the up alignment there and in the surroundings, so that $\delta\langle\sigma(\mathbf{r}_1)\rangle$ and the response function (1.2) are negative. With the same type of arguments or from simply reversing the directions of all the spins, one finds that for a uniform $-$ boundary the response function (1.2) is positive. For either sign of the boundary spins,

Published by the American Physical Society under the terms of the Creative Commons Attribution 4.0 International license. Further distribution of this work must maintain attribution to the author(s) and the published article's title, journal citation, and DOI.

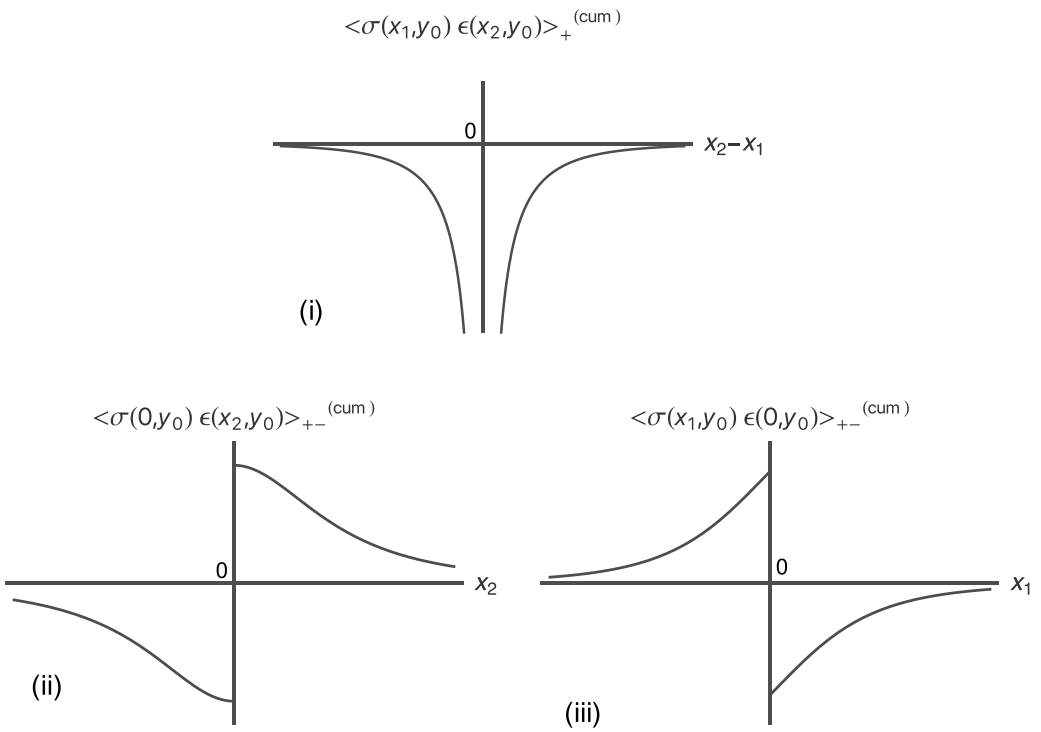


FIG. 1. Sketch of the response function $\langle\sigma\,\epsilon\rangle^{\mathrm{cum}}$ discussed intuitively in paragraphs (i), (ii), and (iii) and by means of the OPE in paragraphs Case (i), Case (ii), and Case (iii) of the Introduction. For the quantitative behaviors of (ii) and (iii) see the red lines in panels (a) and (b) of Fig. 2.

increasing the magnitude of the order at $\mathbf{r}_1$ decreases the disorder at $\mathbf{r}_2$ and increasing the disorder at $\mathbf{r}_2$ decreases the magnitude of the order at $\mathbf{r}_1$.

(ii) What happens for mixed $+-$ boundary conditions [3], where the boundary spins are fixed in the up and down direction along the negative and positive x axis, respectively? Here, the y axis separates regions of positive and negative order and represents a "zero line," along which $\langle\sigma\rangle$ vanishes [3,4]. A local up-ordering imposed at a point $\mathbf{r}_1$ right on the zero line extends into the surroundings on the left and right, generating, by the arguments given in (i), a decrease and increase, respectively, of the disorder at $\mathbf{r}_2$. This leads to an interesting behavior of the response function (1.2), discussed below.

(iii) Placing the point $\mathbf{r}_2$ of disordering right on the zero line leads to another interesting effect. One might guess that the increase in disorder on the zero line extends to both sides of the line, thereby *reducing* the magnitude of the order on both sides, but this is incorrect. The magnitude of the order at $\mathbf{r}_1$ is actually *increased*, as we shall see.

Corresponding explicit results for the response function (1.2) are shown in panels (i), (ii), and (iii) of Fig. 1. Here it is assumed that $\mathbf{r}_1$ and $\mathbf{r}_2$ move on a line $y = y_0$ parallel to the bounding x axis. The behavior is qualitatively in accordance with the above intuitive arguments and displays a remarkable structure at short distance $|\mathbf{r}_{12}|$. The latter seems to have been overlooked despite the fact that it can be obtained from exact results in Ref. [3].

Here we explain how to obtain the short distance behavior without detailed calculations by invoking the OPE [11] of $\sigma\times\epsilon$. For this, only the first two terms of the expansion are needed which read

$$\sigma(\mathbf{r}_1)\,\epsilon(\mathbf{r}_2) \to -\frac{1}{2|\mathbf{r}_{12}|}\big[1+4\,\mathbf{r}_{21}\,\partial_{\mathbf{r}_1}+\cdots\big]\sigma(\mathbf{r}_1)$$
$$\to -\frac{1}{2|\mathbf{r}_{12}|}\big[1-3\,\mathbf{r}_{12}\,\partial_{\mathbf{r}_2}+\cdots\big]\sigma(\mathbf{r}_2). \quad (1.3)$$

The two displayed expressions on the right hand side of (1.3) are equal, apart from higher order terms in the small distance $|\mathbf{r}_{12}|$. This follows from $\sigma(\mathbf{r}_1)\to[1+\mathbf{r}_{12}\,\partial_{\mathbf{r}_2}]\sigma(\mathbf{r}_2)$. There is an important difference between the OPE in (1.3) and those in (1.1). In Eq. (1.1) the leading contributions are given by the nonfluctuating terms $|z_{12}|^{-1/4}$ and $|z_{12}|^{-2}$, which are the same as in the bulk spin-spin and energy-energy correlation functions and which are unperturbed by the boundary conditions or other operators. In Eq. (1.1) these perturbations enter in next-to-leading order, but in the OPE (1.3) they enter in *leading* order [12].

Taking the thermal average of Eq. (1.3), one obtains exact, universal expressions for the short-distance behavior [13] of the response function (1.2) that confirm and extend the above intuitive expectations.

Case (i). For original order $\langle\sigma(\mathbf{r}_1)\rangle > 0$ and $\langle\sigma(\mathbf{r}_1)\rangle < 0$, the first terms on the right-hand side of (1.3) predict $\langle\sigma\epsilon\rangle^{(\mathrm{cum})} < 0$ and $\langle\sigma\epsilon\rangle^{(\mathrm{cum})} > 0$, respectively, in agreement with the intuitive arguments in (i). We also obtain the explicit expression $\langle\sigma(\mathbf{r}_1)\epsilon(\mathbf{r}_2)\rangle_+^{(\mathrm{cum})} \to -\langle\sigma(\mathbf{r}_1)\rangle_+/(2|\mathbf{r}_{12}|)$ for the power-law singularity in the short-distance behavior.

Case (ii). If $\langle\sigma(\mathbf{r}_1)\rangle$ vanishes, the leading behavior for small $|\mathbf{r}_{12}|$ is determined by the second term in (1.3), provided that the first derivative $\partial_{\mathbf{r}_1}\langle\sigma(\mathbf{r}_1)\rangle$ is nonvanishing. In the $+-$

half plane let us place σ right on the zero line, choosing $\mathbf{r}_1 = (x_1, y_1) = (0, y_0)$ [14], and let us place ϵ on the line $y = y_0$. Then, the upper Eq. (1.3) yields

$$\langle \sigma(0, y_0)\, \epsilon(x_2, y_0)\rangle_{+-}^{(\mathrm{cum})} \to 2\,(\mathrm{sgn}\, x_2) \times \left|\left[\partial_{x_1} \langle \sigma(x_1, y_0)\rangle_{+-}\right]_{x_1=0}\right| \tag{1.4}$$

for small $|x_2|$. The signs of $\langle \sigma\, \epsilon\rangle_{+-}^{(\mathrm{cum})}$ in (1.4) are in agreement with the decrease and increase of disorder to the left and right of the zero line, as argued intuitively in (ii). Instead of the power law divergence in (i), the nonanalyticity for $x_2 = x_1$ now has the milder form of an upward jump in sign as x_2 grows. Later on we shall consider cases where both $\langle\sigma\rangle$ and its first derivative vanish, leading to an even milder form of nonanalyticity.

Case (iii). For ϵ right on the y axis, i.e., $\mathbf{r}_2 = (x_2, y_2) = (0, y_0)$, the lower form of Eq. (1.3) yields a *downward* jump in sign

$$\langle \sigma(x_1, y_0)\, \epsilon(0, y_0)\rangle_{+-}^{(\mathrm{cum})} \to -(3/2)\,(\mathrm{sgn}\, x_1) \times \left|\left[\partial_{x_2} \langle \sigma(x_2, 0)\rangle_{+-}\right]_{x_2=0}\right| \tag{1.5}$$

as the position x_1 of σ increases along the line $y = y_0$. Thus, increasing the disorder right on the defect line *enhances* the up-order to its left and the down-order to its right. The reason is that near the y axis, where the sign of $\langle\sigma\rangle_{+-}$ changes, the disorder is large. Further increasing the disorder facilitates the sign change and leads to the enhancement. This argument is made more explicit in Ref. [15].

While the upward and downward jumps depend on the value of the first derivative $\partial\langle\sigma\rangle$ this drops out from their ratio $2/(-3/2) = -4/3$ which is universal, i.e., the same for crossing other zero lines of $\langle\sigma\rangle$. Examples are presented in Secs. IV and V.

So far we have only analyzed the response function $\langle\sigma(\mathbf{r}_1)\epsilon(\mathbf{r}_2)\rangle$ for short distances between $\mathbf{r}_1$ and $\mathbf{r}_2$. In Secs. II–V we study the response function for arbitrary $\mathbf{r}_1$ and $\mathbf{r}_2$ in some Ising systems with uniform and mixed boundary conditions for which exact results [3,4] are available. These include the upper half planes with $+$, $+-$, and $-+-$ boundary conditions and a finite equilateral triangle with $-+-$ boundaries. This gives us the opportunity to confirm that the response function not only obeys the OPE in Eq. (1.3) and its extension to higher order in Appendix A but also the "boundary-operator expansion" BOE [1,2,5] and the "corner-operator expansion" COE [6].

Finally, in Sec. VI we consider a square with $+$ spins on the horizontal boundaries and $-$ spins on the vertical boundaries, at the center of which both $\langle\sigma\rangle$ and its first derivatives vanish. Here the OPE predicts that the leading short-distance singularities of the response function have a cusplike form.

II. UPPER HALF PLANE WITH A UNIFORM BOUNDARY CONDITION +

In the upper half plane with uniform boundary condition $+$ the two point function reads

$$\langle\sigma(1)\,\epsilon(2)\rangle_+ = \langle\sigma(1)\rangle_+\,\langle\epsilon(2)\rangle_+ \times \frac{1}{|\mathbf{r}_{12}|}\,\frac{(x_1-x_2)^2 + y_1^2 + y_2^2}{\sqrt{(x_1-x_2)^2 + (y_1+y_2)^2}},$$
$$\langle\sigma(1)\rangle_+ = (2/y_1)^{1/8}, \quad \langle\epsilon(2)\rangle_+ = -1/(2y_2), \quad |\mathbf{r}_{12}| = \sqrt{(x_1-x_2)^2 + (y_1-y_2)^2}. \tag{2.1}$$

See Ref. [3]. For short we denote here $\mathbf{r}_1 = (x_1, y_1)$ and $\mathbf{r}_2 = (x_2, y_2)$ by 1 and 2, respectively. For $|\mathbf{r}_{12}| \to 0$ the two-point function approaches

$$\langle\sigma(1)\,\epsilon(2)\rangle_+ \to -\langle\sigma(1)\rangle_+ \times \frac{1}{2|\mathbf{r}_{12}|}, \tag{2.2}$$

consistent with the OPE (1.3) and panel (i) in Fig. 1, and for $|\mathbf{r}_{12}| \to \infty$ with y_1, y_2 fixed it approaches $\langle\sigma(1)\rangle_+\langle\epsilon(2)\rangle_+[1 + 2(y_1y_2/|\mathbf{r}_{12}|^2)^2]$, consistent with the BOE [16] together with the form $\langle T(x_1)T(x_2)\rangle_+ = 1/[4(x_1-x_2)^4]$ of the TT cumulant in the boundary. Here $T(z)$ is the stress tensor [2].

For later comparison we note the corresponding cumulant along the horizontal axis $y = y_0$

$$\langle\sigma(x_1, y_0)\,\epsilon(x_2, y_0)\rangle_+^{(\mathrm{cum})} = -\frac{2^{(1/8)-1}}{y_0^{(1/8)+1}} \times \left[|X_{21}|^{-1}\left(X_{21}^2+4\right)^{-1/2}\left(X_{21}^2+2\right) - 1\right], \tag{2.3}$$

where $X_{21} = (x_2 - x_1)/y_0$. It is an even function of X_{21} that, starting from $-\infty$, monotonically increases to 0 when $|X_{21}|$ increases from 0 to ∞. Correspondingly the odd second term in the OPE (1.3) is absent since $\partial_{x_1}\langle\sigma(1)\rangle_+$ vanishes.

This is different along the vertical axis $x = 0$ where

$$\langle\sigma(x_1 = 0, y_1)\,\epsilon(x_2 = 0, y_2)\rangle_+ = \langle\sigma(1)\rangle_+\,\langle\epsilon(2)\rangle_+ \times \frac{y_1^2 + y_2^2}{|y_1^2 - y_2^2|}. \tag{2.4}$$

Here both even and odd powers of y_{21} appear and the nonvanishing second term in (1.3) is reproduced. It is rewarding to check the consistency between (2.4) and the OPE to higher order. This is done up to order $y_{21}^3/|y_{21}|$ in Appendix A 3.

III. UPPER HALF PLANE WITH A +− BOUNDARY CONDITION

The upper half $z = x + iy$ plane with boundary condition + for $x < 0$ and − for $x > 0$ is perhaps the simplest geometry that displays the features mentioned in paragraphs (ii) and (iii) in the Introduction. For the present +− boundary condition we can use the explicit form of the response function derived by Burkhardt and Xue; see Eqs. (4.1) and (4.3) in Ref. [3]. First note its basic symmetry

$$\langle\sigma(x_1,y_1)\,\epsilon(x_2,y_2)\rangle_{+-}^{(\mathrm{cum})} = -\langle\sigma(-x_1,y_1)\,\epsilon(-x_2,y_2)\rangle_{+-}^{(\mathrm{cum})}, \tag{3.1}$$

which implies, in particular, that it vanishes for $x_1 = x_2 = 0$. Now consider the response function along the line $y = y_0$ with one of the two operators on the zero line $x = 0$, i.e., $x_1 = 0$, x_2 arbitrary [case (i)] and $x_2 = 0$, x_1 arbitrary [case (ii)].

In case (i), $\langle\sigma\rangle_{+-}$ vanishes and one finds

$$\langle\sigma(0,y_0)\,\epsilon(x_2,y_0)\rangle_{+-}^{(\mathrm{cum})} = \frac{2^{(1/8)-1}}{y_0^{(1/8)+1}} \times 4\left(1+\frac{X_2^2}{4}\right)^{-1/2}\left(1+X_2^2\right)^{-1}\mathrm{sgn}X_2, \tag{3.2}$$

where $X_2 \equiv x_2/y_0$ and, for comparison, we have used the same prefactor as in (2.3). In accordance with (3.1), Eq. (3.2) is odd in X_2 and it shows the limiting behaviors

$$\langle\sigma(0,y_0)\,\epsilon(x_2,y_0)\rangle_{+-}^{(\mathrm{cum})} \to \frac{2^{(1/8)-1}}{y_0^{(1/8)+1}} \times 4\left\{(\mathrm{sgn}X_2)\left(1-\frac{9}{8}X_2^2\right),\ \frac{2}{X_2^3}\right\} \tag{3.3}$$

for $|X_2| \to \{0,\ \infty\}$. These are in agreement with the predictions of the {OPE, BOE}. For the OPE prediction in leading order see Eq. (1.4) together with (A20) and in next-to-leading order see Eq. (A23). For the BOE prediction see (B7) together with Ref. [16].

In case (ii) the result is

$$\begin{aligned}\langle\sigma(x_1,y_0)\,\epsilon(0,y_0)\rangle_{+-}^{(\mathrm{cum})} = &-\frac{2^{(1/8)-1}}{y_0^{(1/8)+1}} \times 3\left(1+\frac{X_1^2}{2}\right)\left(1+\frac{X_1^2}{4}\right)^{-1/2}\\ &\times\left(1+X_1^2\right)^{-1/2}\mathrm{sgn}X_1 \;-\; \langle\sigma(x_1,y_0)\rangle_{+-} \times \langle\epsilon(0,y_0)\rangle_{+-},\end{aligned} \tag{3.4}$$

where

$$\langle\sigma(x_1,y_0)\rangle_{+-} = -\left(\frac{2}{y_0}\right)^{1/8}\left(1+X_1^2\right)^{-1/2}X_1, \quad \langle\epsilon(0,y_0)\rangle_{+-} = \frac{3}{2y_0}, \tag{3.5}$$

and where $X_1 = x_1/y_0$. The two contributions to the cumulant, the two-point function $\langle\sigma\epsilon\rangle_{+-}$ and the subtracted product of one-point functions $-\langle\sigma\rangle_{+-} \times \langle\epsilon\rangle_{+-}$, are both odd in X_1 and for $|X_1| \to \infty$ there is a cancellation so that the right-hand side (RHS) of (3.4) tends to the product of $-2^{(1/8)-1}/y_0^{(1/8)+1}$ and $6(\mathrm{sgn}X_1)/X_1^4$. Near $X_1 = 0$, where the operator positions coincide, the behavior of the two contributions is quite different: while the two-point function is nonanalytic as required by the OPE, the product of one-point functions is analytic and not related to the OPE.

The behavior of $\langle\sigma\epsilon\rangle_{+-}^{(\mathrm{cum})}$ given in Eqs. (3.2)–(3.5) is entirely different from its counterpart for a uniform + boundary given in (2.3). On the other hand, for $x_1 \to -\infty$ with $x_2 - x_1 = y_0 X_{21}$ fixed, $\langle\sigma(x_1,y_0)\,\epsilon(x_2,y_0)\rangle_{+-}^{(\mathrm{cum})}$ must approach the form of (2.3) which is sketched in panel (i) of Fig. 1. This happens in an interesting way as shown in Fig. 2.

The expression of the response function for *arbitrary* positions of σ and ϵ follows from Eq. (4.3) in Ref. [3] and can be written as [17]

$$\langle\sigma(x_1,y_1)\,\epsilon(x_2,y_2)\rangle_{+-}^{(\mathrm{cum})} = -\frac{2^{(1/8)-1}}{y_1^{1/8}\,y_2} \times \frac{1}{|z_1|\,|z_2|^2}\left[\frac{A+B+C}{|z_1-z_2|\,|z_1-\bar{z}_2|} - \left(|z_2|^2 - z_2^2 - \bar{z}_2^2\right)\frac{z_1+\bar{z}_1}{2}\right], \tag{3.6}$$

where

$$\begin{aligned}A &= \left(|z_1|^2+|z_2|^2\right)\left(|z_2|^2 - z_2^2 - \bar{z}_2^2\right)\frac{z_1+\bar{z}_1}{2},\\ B &= \frac{1}{2}\left(z_1-\bar{z}_1\right)^2|z_2|^2\,\frac{z_2+\bar{z}_2}{2},\\ C &= |z_1|^2\left(z_2^3+\bar{z}_2^3\right)\end{aligned} \tag{3.7}$$

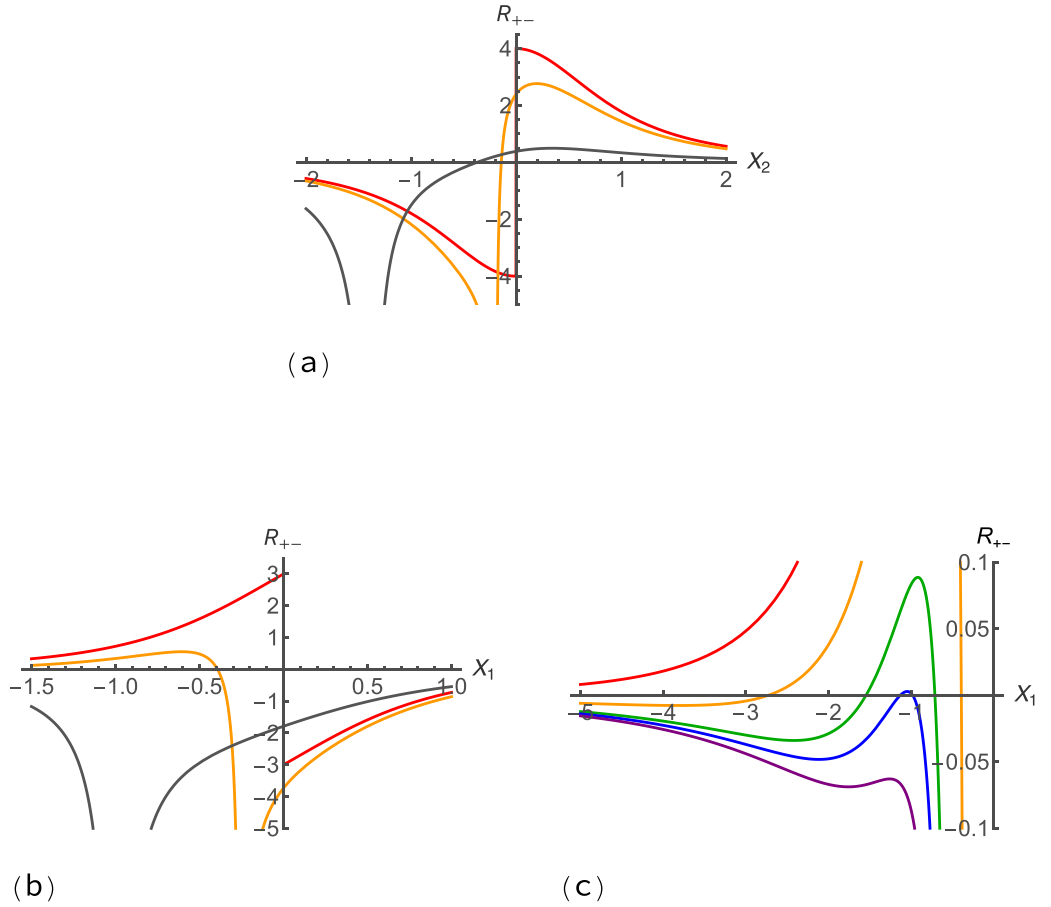


FIG. 2. Dimensionless response function $R_{+-} \equiv R_{+-}(X_1, X_2)$ along a line parallel to the x axis in the upper half x, y plane with $+-$ boundary condition as given in Eq. (3.8). The red, orange, and gray curves in panel (a) show the X_2 dependence for X_1 fixed at 0, -0.2, -1.4, while in panel (b) they show the X_1 dependence for X_2 fixed at 0, -0.25, -1. For fixing X_1 and X_2 at 0 the upward and downward jumps, $4\,\mathrm{sgn}X_2$ and $-3\,\mathrm{sgn}X_1$ appearing in panels (a) and (b), respectively, are consistent with Eqs. (1.4) and (1.5) since $|\partial_x \langle\sigma(x, y_0)\rangle_{+-}|_{x=0} = 2^{1/8}/y_0^{(1/8)+1}$; see Eq. (A20). On decreasing the fixed positions of X_1 and X_2 in panels (a) and (b), respectively, the corresponding X_2 and X_1 dependencies tend towards the $|X_2 - X_1|$ dependence for a uniform $+$ boundary given in Eq. (2.3) and shown in panel (i) of Fig. 1. In particular, the "disordering *enhances* order" regions addressed in paragraph (iii) of the Introduction that appear in (b) as $R_{+-} > 0$ for $X_1 < 0$ decrease and vanish as the fixed locations X_2 of ϵ decrease from 0 via -0.25 to -1, so that $\langle\sigma\epsilon\rangle^{(\mathrm{cum})}$ becomes negative for all $X_1 < 0$. The complexity of this process is displayed in more detail in panel (c) which shows the X_1 dependences for X_2 fixed at 0, -0.25, -0.36, -0.39, and -0.42 in red, orange, green, blue, and purple: all curves with X_2 fixed must approach zero as $X_1 \to -\infty$. While for $X_2 = 0$ (red curve) the approach is from above, see the remark below (3.5), for all $X_2 < 0$ the approach is from below.

and the second term in the square bracket in (3.6) arises from subtracting the product of one-point functions. Along the line $y = y_0$ this yields the expression

$$R_{+-}(X_1, X_2) \equiv \left(y_0^{(1/8)+1}/2^{(1/8)-1}\right) \langle\sigma(x_1, y_0)\,\epsilon(x_2, y_0)\rangle_{+-}^{(\mathrm{cum})}$$
$$= \frac{1}{\sqrt{X_1^2+1}\,(X_2^2+1)} \left\{ \frac{X_1(X_2^2-3)\left[X_1^2+X_2^2-2X_1X_2+2\right]+8X_2}{|X_1-X_2|\sqrt{(X_1-X_2)^2+4}} - X_1(X_2^2-3) \right\}, \quad X_1 \equiv x_1/y_0,\ X_2 \equiv x_2/y_0 \tag{3.8}$$

on which Fig. 2 is based. The RHS of (3.8) obeys the antisymmetry (3.1) and in the limit $X_1 \to -\infty$ with $X_2 - X_1$ fixed it reduces to the expression (2.3) for a uniform $+$ boundary.

IV. BOUNDARY CONDITION $-+-$

Here we consider the two point function $\langle\sigma\epsilon\rangle_{-+-}$ and its cumulant in the upper half $h = g + ij$ plane with boundary conditions $-$ for $g < -1$, $+$ for $-1 < g < 1$, and $-$ for $g > 1$. This function is symmetric about the imaginary axis $g = 0$,

i.e.,

$$\langle\sigma(g_1, j_1)\,\epsilon(g_2, j_2)\rangle_{+-}^{(\mathrm{cum})} = \langle\sigma(-g_1, j_1)\,\epsilon(-g_2, j_2)\rangle_{+-}^{(\mathrm{cum})}, \tag{4.1}$$

which should be compared with the antisymmetry (3.1) for the $+-$ boundary.

The present two point function $\langle\sigma\epsilon\rangle_{-+-}$ in the h plane is related to the two point function $\langle\sigma\epsilon\rangle_{+-}$ in the z plane contained in Eqs. (3.6) and (3.7) by means of the Möbius transformation

$$z(h) = \frac{h-1}{h+1}, \quad \frac{dz}{dh} = \frac{2}{(h+1)^2}. \tag{4.2}$$

The result is

$$\langle\sigma(g_1, j_1)\,\epsilon(g_2, j_2)\rangle_{-+-} = -\frac{1}{2j_2}\left(\frac{2}{j_1}\right)^{1/8} \frac{a+b+c}{4|h_1-h_2|\,|h_1-\bar{h}_2|}, \tag{4.3}$$

where

$$\begin{aligned} a &= \frac{|h_1|^2-1}{|h_1^2-1|}\,[|h_1-1|^2\,|h_2+1|^2 + (h_1 \leftrightarrow h_2)]\,(1-2\,\cos(2\Phi_2)),\\ b &= \frac{2(h_1-\bar{h}_1)^2\,(|h_2|^2-1)}{|h_1^2-1|},\\ c &= |h_1^2-1|\,|h_2^2-1|2\,\cos(3\Phi_2). \end{aligned} \tag{4.4}$$

Here

$$\Phi_2 \equiv \arg(h_2-1) - \arg(h_2+1), \tag{4.5}$$

and $\cos(2\Phi_2)$ and $\cos(3\Phi_2)$ arise from rewriting

$$\begin{aligned} (h_2-1)^2\,(\bar{h}_2+1)^2 + \text{c.c.} &= |h_2^2-1|^2\,2\,\cos(2\Phi_2),\\ \frac{(h_2-1)^2\,(\bar{h}_2+1)^2}{(h_2+1)\,(\bar{h}_2-1)} + \text{c.c.} &= |h_2^2-1|\,2\,\cos(3\Phi_2) \end{aligned} \tag{4.6}$$

of terms that appear in the course of the transformation.

The expression for the cumulant $\langle\sigma\epsilon\rangle_{-+-}^{(\mathrm{cum})} \equiv \langle\sigma\epsilon\rangle_{-+-} - \langle\sigma\rangle_{-+-} \times \langle\epsilon\rangle_{-+-}$ follows from Eqs. (4.3)–(4.6) and the forms

$$\langle\sigma(g, j)\rangle_{-+-} = -\left(\frac{2}{j}\right)^{1/8} \times C, \quad \langle\epsilon(g, j)\rangle_{-+-} = -\frac{1}{2j}\,(4C^2-3), \quad C \equiv \frac{|h|^2-1}{|h^2-1|} \tag{4.7}$$

of the one-point functions or profiles of σ and ϵ in the upper $-+-$ half plane. They follow from their counterparts in the $+-$ plane given in Eq. (4.1) in Ref. [3]; see Eqs. (2.14) and (2.23) in Ref. [6]. The zero line with vanishing $\langle\sigma\rangle_{-+-}$ is the upper half unit circle which is the preimage of the imaginary axis in the $+-$ plane. In particular, the point $h = i$ on the zero line is the preimage of $z = i$.

On mirror imaging both points about the imaginary axis in the z plane each of the terms (A, B, C) in (3.7) is antisymmetric while each of the terms (a, b, c) in (4.4) is symmetric in the h plane. Together with the symmetry of the corresponding denominators and the profiles in Eq. (4.7) this leads to the antisymmetry (3.1) and symmetry (4.1) of the cumulants in the z and h plane, respectively. We note that $(A, B, C) = (a, b, c) \times |h_1-1||h_2-1|^2|h_1+1|^{-3}|h_2+1|^{-4}$ on using the relation (4.2).

Consider now the cases in which one of the two operators σ and ϵ is located on a point of the zero line. Here we choose the point $h = i$.

(a) $h_1 = i$. Here Eqs. (4.3)–(4.6) imply

$$\langle\sigma(g_1 = 0, j_1 = 1)\,\epsilon(g_2, j_2)\rangle_{-+-} = 2^{(1/8)+3}\,j_2\,\frac{|h_2|^2-1}{|h_2^2+1|\,|h_2^2-1|^2} \tag{4.8}$$

and we note the corresponding form

$$\langle\sigma(g_1 = 0, j_1 = 1)\,T(h)\rangle_{-+-} = 2^{1/8}\,\frac{2}{h^4-1} \tag{4.9}$$

of $\langle\sigma\,T(h)\rangle_{-+-}$ that follows from subjecting (B7) with $y_0 = 1$ to the transformation (4.2). The near-boundary behavior $j_2 \to 0$ of (4.8) is given by $2^{(1/8)+3}\,j_2/(g_2^4-1)$, which equals the product of $4j_2$ and (4.9) for $h = g_2$, as predicted by the BOE [16]. We also note the expansion of (4.8) for small $|h_2-h_1| \equiv |h_{21}| = \sqrt{g_2^2+(j_2-1)^2}$,

$$\langle\sigma(g_1 = 0, j_1 = 1)\,\epsilon(g_2, j_2)\rangle_{-+-} \to 2^{(1/8)+1}\,\frac{1}{|h_{21}|}\left\{(j_2-1) + \left[\frac{1}{2}g_2^2 - (j_2-1)^2\right] - \frac{7}{8}\,g_2^2\,(j_2-1) + O(|h_{21}|^4)\right\}. \tag{4.10}$$

The first, second, and third term in the curly bracket of (4.10) is consistent with the OPE expressions given in (1.3), (A27), and (A28), respectively. For $g_2 = 0$ Eq. (4.8) takes the simple form

$$\langle\sigma(g_1 = 0,\, j_1 = 1)\,\epsilon(g_2 = 0,\, j_2)\rangle_{-+-} = 2^{(1/8)+3}\,\frac{j_2\,\mathrm{sgn}(j_2 - 1)}{\left(j_2^2 + 1\right)^2} \tag{4.11}$$

displaying the remarkable behavior

$$\langle\sigma(g_1 = 0,\, j_1 = 1)\,\epsilon(g_2 = 0,\, j_2)\rangle_{-+-} \to 2^{(1/8)+1}\left[-4j_2,\ \mathrm{sgn}(j_2 - 1) - |j_2 - 1|,\ 4j_2^{-3}\right] \tag{4.12}$$

for $[j_2 \to 0,\ |j_2 - 1| \ll 1,\ j_2 \gg 1]$ with a discontinuity at $j_2 = 1$ and a prominent minimum at $j_2 = 0.58$, where (4.11) takes the value $-2^{(1/8)+1} \times 1.3$. Unlike Eq. (3.2) where the antisymmetry (3.1) allows only contributions odd in X_2, in (4.11) there is no symmetry in the j direction about the zero $j_1 = 1$ of $\langle\sigma\rangle_{-+-}$ and both odd and even powers in $j_2 - 1$ are present in the expansion which follows from (4.10) or (A26)–(A28). In the last paragraph of Sec. II and in Eq. (A13)ff we encountered this same phenomenon along the vertical y axis of the upper half plane with a uniform + boundary.

(b) $h_2 = i$. Here Eqs. (4.3)–(4.6) imply

$$\langle\sigma(g_1,\, j_1)\,\epsilon(g_2 = 0,\, j_2 = 1)\rangle_{-+-} = -\frac{3}{2}\left(\frac{2}{j_1}\right)^{1/8}\frac{|h_1|^4 - 1}{|h_1^4 - 1|}. \tag{4.13}$$

Equations (4.8) and (4.13) are invariant against $h_2 \to -\bar{h}_2$ and $h_1 \to -\bar{h}_1$, respectively, reflecting the mirror symmetry (4.1). From Eq. (4.13) follows the short distance behavior

$$\begin{aligned}\langle\sigma(g_1 = 0,\, j_1)\,\epsilon(g_2 = 0,\, j_2 = 1)\rangle_{-+-} &\equiv -\tfrac{3}{4}\,2^{(1/8)+1}\,j_1^{-1/8}\,\mathrm{sgn}(j_1 - 1)\\ &\to -\tfrac{3}{4}\,2^{(1/8)+1}\,[\mathrm{sgn}(j_1 - 1) - (1/8)\,|j_1 - 1| + O((j_1 - 1)^2)],\end{aligned} \tag{4.14}$$

which should be compared with the short distance behavior in Eq. (4.12) and which is consistent with the OPE expression in (A29). Subtracting the expanded product of one-point functions given in (4.7) then yields

$$\langle\sigma(g_1 = 0,\, j_1)\,\epsilon(g_2 = 0,\, j_2 = 1)\rangle_{-+-}^{(\mathrm{cum})} \to -\tfrac{3}{4}\,2^{(1/8)+1}\,[\mathrm{sgn}(j_1 - 1) - (1/8)\,|j_1 - 1| - (j_1 - 1) + O((j_1 - 1)^2)] \tag{4.15}$$

for the cumulant.

Behavior of $\langle\sigma\,\epsilon\rangle_{-+-}^{\mathrm{cum}}$ for arbitrary points on the symmetry axis

For both σ and ϵ positioned at arbitrary points on the imaginary axis of the h plane, i.e., for $g_1 = g_2 = 0$, Eqs. (4.3)ff yield for the cumulant

$$\begin{aligned}\langle\sigma(g_1 = 0,\, j_1)\,\epsilon(g_2 = 0,\, j_2)\rangle_{-+-}^{(\mathrm{cum})} &= -\frac{1}{2j_2}\left(\frac{2}{j_1}\right)^{1/8}\mathscr{A}\left(j_1^2,\, j_2^2\right),\\ \mathscr{A}(p, q) &\equiv \frac{2}{|p - q|(p + 1)(q + 1)^2}[q(1 + 15p - 14q - 2pq + q^2 - pq^2),\, p(1 - p + 2q + 14pq - 15q^2 - pq^2)]\end{aligned} \tag{4.16}$$

for $[q < p,\ p < q]$. The antisymmetry about the imaginary axis in the z plane addressed in Sec. III translates along the present imaginary axis in the h plane to an inversion antisymmetry of $\mathscr{A}$ about $h = i$ so that

$$\mathscr{A}(p^{-1},\, q^{-1}) \,=\, -\mathscr{A}(p,\, q). \tag{4.17}$$

The special cases

$$\mathscr{A}(1, q) = -\frac{16q}{(q + 1)^2} \times \mathrm{sgn}(q - 1), \quad \mathscr{A}(p, 1) = 3\left[\mathrm{sgn}(p - 1) - \frac{p - 1}{p + 1}\right] \tag{4.18}$$

serve to rederive the cumulant expansions (4.12), (4.15) for $(j_1 = 1,\ j_2 \to 1)$, $(j_2 = 1,\ j_1 \to 1)$. The universal ratio $-4/3$ mentioned in the Introduction after Eq. (1.5) immediately follows from the leading terms for $q \to 1$, $p \to 1$ in (4.18).

For later use we note the limiting behaviors

$$\langle\sigma(g_1 = 0,\, j_1)\,\epsilon(g_2 = 0,\, j_2)\rangle_{-+-}^{(\mathrm{cum})} \to \left(\frac{2}{j_1}\right)^{1/8}\frac{1}{j_1^2 + 1}\left\{-\frac{j_2\left(15j_1^2 + 1\right)}{j_1^2},\ \frac{j_1^2\left(j_1^2 + 15\right)}{j_2^3}\right\} \tag{4.19}$$

for $\{j_2 \to 0,\ j_2 \to \infty\}$ and

$$\langle\sigma(g_1 = 0,\, j_1)\,\epsilon(g_2 = 0,\, j_2)\rangle_{-+-}^{(\mathrm{cum})} \to \left(\frac{2}{j_1}\right)^{1/8}\frac{1}{\left(j_2^2 + 1\right)^2}\left\{\frac{j_1^2\left(15j_2^4 - 2j_2^2 - 1\right)}{j_2^3},\ \frac{j_2\left(j_2^4 + 2j_2^2 - 15\right)}{j_1^2}\right\} \tag{4.20}$$

for $\{j_1 \to 0,\ j_1 \to \infty\}$.

Here it is useful to make contact with the cumulants containing the stress tensor discussed in Appendix B. For j_1 arbitrary fixed and j_2 tending either to 0 or to ∞ one finds

$$\langle\sigma(g_1=0,\,j_1)\,\epsilon(g_2=0,\,j_2)\rangle^{(\mathrm{cum})}_{-+-}\big/\langle\sigma(g_1=0,\,j_1)\,T(h=ij_2)\rangle^{(\mathrm{cum})}_{-+-}\;\to\;4j_2, \tag{4.21}$$

while for j_2 arbitrary fixed and j_1 tending either to 0 or to ∞

$$\langle\sigma(g_1=0,\,j_1)\,\epsilon(g_2=0,\,j_2)\rangle^{(\mathrm{cum})}_{-+-}\big/\langle T(h=ij_1)\,\epsilon(g_2=0,\,j_2)\,\rangle^{(\mathrm{cum})}_{-+-}\to\;\{-,+\}\left(\frac{2}{j_1}\right)^{1/8}j_1^2. \tag{4.22}$$

This follows by comparing Eqs. (4.19) with the corresponding limiting behaviors of $\langle\sigma\,T\rangle^{(\mathrm{cum})}_{-+-}$ given in Eqs. (B12) and, likewise, Eq. (4.22) with (B14). For $j_2\to 0$ and $j_1\to 0$, where ϵ and σ, respectively, approach the boundary the relations confirm the BOE [16].

In our discussion of a triangle in Sec. V we shall use the properties (4.21) and (4.22) for $j_2\to\infty$ and $j_1\to\infty$ to show that on approaching a corner of the triangle the behavior is consistent with the "corner operator expansion" COE [18].

V. EQUILATERAL TRIANGLE WITH − + − BOUNDARY CONDITION

Here we consider the critical behavior inside an equilateral triangle in the $z=x+iy$ plane with side length $\mathscr{W}$, with corners at

$$z=z_{\mathrm{A}}=-\mathscr{W}/2,\quad z_{\mathrm{B}}=\mathscr{W}/2,\quad z_{\mathrm{C}}=i(\sqrt{3}/2)\mathscr{W}=iy_{\mathrm{C}}, \tag{5.1}$$

and with boundary conditions + along the horizontal AB side and − along the CA and CB sides. Correlation functions can be related to those in the upper half $h=g+ij$ plane described in Sec. IV by means of the conformal transformation $h(Z)$ in Appendix C. Here one uses the dimensionless variable $Z=X+iY$ defined in Eq. (C1) which measures the position z conveniently in terms of the side length $\mathscr{W}$ or the height $y_{\mathrm{C}}=(\sqrt{3}/2)\mathscr{W}$ of the triangle. The relation for our $\sigma\times\epsilon$ cumulant then reads

$$\langle\sigma(x_1,\,y_1)\,\epsilon(x_2,\,y_2)\rangle^{(\mathrm{cum})}_{\mathrm{triangle}}=\left(\frac{Y_{\mathrm{C}}}{y_{\mathrm{C}}}\right)^{(1/8)+1}|S(Z_1)|^{1/8}\,|S(Z_2)|\,\langle\sigma(g_1,\,j_1)\,\epsilon(g_2,\,j_2)\rangle^{(\mathrm{cum})}_{-+-},\quad S(Z)\equiv\frac{dh}{dZ}. \tag{5.2}$$

Here $Y_{\mathrm{C}}=3.196284004$ is the Y argument of the upper corner; see Eq. (C8).

It is instructive to consider the behavior along the vertical midline $Z=iY,\;0<Y<Y_{\mathrm{C}}$ of the triangle which is mapped to the midline $h=ij,\;0<j<\infty$ of the half plane system in Sec. IV. The explicit expressions of $S(iY)=|S(iY)|$ and $j(Y)$ are given in Eqs. (C9) and (C6), respectively. We note the form

$$\langle\sigma(x=0,\;y)\rangle_{\mathrm{triangle}}\;=\left(\frac{Y_{\mathrm{C}}}{y_{\mathrm{C}}}\right)^{1/8}\times S(iY)^{1/8}\times\left(\frac{2}{j}\right)^{1/8}\times\frac{1-j^2}{1+j^2} \tag{5.3}$$

of the one-point function $\langle\sigma\rangle_{\mathrm{triangle}}$ along the midline which follows from Eq. (4.7). It vanishes for $Y=Y_0\equiv 0.74326$ since this corresponds to $j=1$, see Eq. (C8), and it is positive and negative for $Y<Y_0$ and $Y>Y_0$, respectively.

First we discuss the behavior of the response function (5.2) when ϵ or σ approach the base line or the upper corner of the triangle. Boundary operator expansions serve for a deeper understanding of what happens when a bulk operator approaches a flat boundary or corner [1,2,5,6]. Like in Sec. IV and Appendix B we relate the average (5.2) of $\sigma\times\epsilon$ along the midline to the corresponding averages of $\sigma\times T$ and $T\times\epsilon$. These read

$$\langle\sigma(x_1=0,\,y_1)\,T(iy_2)\rangle^{(\mathrm{cum})}_{\mathrm{triangle}}=\left(\frac{Y_{\mathrm{C}}}{y_{\mathrm{C}}}\right)^{(1/8)+2}S(iY_1)^{1/8}\,S^2(iY_2)\,\langle\sigma(g_1=0,\,j_1)T(ij_2)\rangle^{(\mathrm{cum})}_{-+-} \tag{5.4}$$

and

$$\langle T(iy_1)\,\epsilon(x_2=0,\,y_2)\,\rangle^{(\mathrm{cum})}_{\mathrm{triangle}}=\left(\frac{Y_{\mathrm{C}}}{y_{\mathrm{C}}}\right)^{2+1}S(iY_1)^2\,S(iY_2)\,\langle T(ij_1)\,\epsilon(g_2=0,\,j_2)\rangle^{(\mathrm{cum})}_{-+-}, \tag{5.5}$$

respectively, and we find the ratios

$$\frac{\langle\sigma(x_1=0,\,y_1)\,\epsilon(x_2=0,\,y_2)\rangle^{(\mathrm{cum})}_{\mathrm{triangle}}}{\langle\sigma(x_1=0,\,y_1)\,T(iy_2)\rangle^{(\mathrm{cum})}_{\mathrm{triangle}}}\to\frac{y_{\mathrm{C}}}{Y_{\mathrm{C}}}\,\frac{4j(Y_2)}{R(iY_2)}\;\to\;4\{y_2,\;(y_{\mathrm{C}}-y_2)/3\} \tag{5.6}$$

and

$$\begin{aligned}\frac{\langle\sigma(x_1=0,\,y_1)\,\epsilon(x_2=0,\,y_2)\rangle^{(\mathrm{cum})}_{\mathrm{triangle}}}{\langle T(iy_1)\,\epsilon(x_2=0,\,y_2)\rangle^{(\mathrm{cum})}_{\mathrm{triangle}}}\;&\to\;\{-,\,+\}\,2^{1/8}\left(\frac{y_{\mathrm{C}}}{Y_{\mathrm{C}}}\,\frac{j(Y_1)}{R(iY_1)}\right)^{2-(1/8)}\\&\to\;2^{1/8}\left\{-y_1^{2-(1/8)},\;[(y_{\mathrm{C}}-y_1)/3]^{2-(1/8)}\right\}\end{aligned} \tag{5.7}$$

in the limits $\{y_2 \to 0,\ y_2 \to y_C\}$ and $\{y_1 \to 0,\ y_1 \to y_C\}$, respectively. To derive (5.6) and (5.7) we have used Eqs. (4.21) and (4.22) in the first steps and Eqs. (C12) and (C13) in the second steps. That the ratios in (5.6) and (5.7) are *independent* of y_1 and y_2, respectively, and have the simple forms given on their right-hand sides are important consequences of the BOE explained in [16] and of the COE [18] on using relations given in Eqs. (4.5) in Ref. [6].

Now we discuss the above limiting behaviors for the response function in the numerators of (5.6) and (5.7) which do depend on y_1 and y_2, respectively. Using the short notation

$$\langle \sigma(x_1 = 0, y_1)\, \epsilon(x_2 = 0, y_2)\rangle^{(\mathrm{cum})}_{\mathrm{triangle}} \equiv \mathscr{R}(y_1,\ y_2) \tag{5.8}$$

for the response function they read

$$\begin{aligned} \mathscr{R}(y_1,\ y_2) &\to \left(\frac{Y_C}{y_C}\right)^{(1/8)+1} 3^{3/2} \times (Y_2/4) \times \mathscr{B}_2(Y_1), \\ \mathscr{B}_2(Y_1) &= -\left[3^{3/4}\left(1 + j_1^2\right)^{2/3}/j_1\right]^{1/8} \frac{15 j_1^2 + 1}{j_1^2\left(j_1^2 + 1\right)} \end{aligned} \tag{5.9}$$

and

$$\begin{aligned} \mathscr{R}(y_1,\ y_2) &\to \left(\frac{Y_C}{y_C}\right)^{(1/8)+1} \frac{1}{2} 3^{-1/2} \times (\delta_2/2)^5 \times \mathscr{C}_2(Y_1), \\ \mathscr{C}_2(Y_1) &= \left[3^{3/4}\left(1 + j_1^2\right)^{2/3}/j_1\right]^{1/8} \frac{j_1^2\left(j_1^2 + 15\right)}{j_1^2 + 1} \end{aligned} \tag{5.10}$$

for $y_2 \to 0$ and $y_2 \to y_C$, respectively. For $y_1 \to 0$ and $y_1 \to y_C$ the result is

$$\begin{aligned} \mathscr{R}(y_1,\ y_2) &\to \left(\frac{Y_C}{y_C}\right)^{(1/8)+1} 3^{3/2} \times (Y_1/2)^{2-(1/8)} \times \mathscr{B}_1(Y_2), \\ \mathscr{B}_1(Y_2) &= \frac{1}{2} 3^{3/4}\left(1 + j_2^2\right)^{2/3} \frac{15 j_2^4 - 2 j_2^2 - 1}{j_2^3\left(j_2^2 + 1\right)^2} \end{aligned} \tag{5.11}$$

and

$$\begin{aligned} \mathscr{R}(y_1,\ y_2) &\to \left(\frac{Y_C}{y_C}\right)^{(1/8)+1} 3^{-11/8} (\delta_1/2)^{6-(1/8)} \times \mathscr{C}_1(Y_2), \\ \mathscr{C}_1(Y_2) &= \frac{1}{2}\, 3^{3/4}\left(1 + j_2^2\right)^{2/3} \frac{j_2\left(j_2^4 + 2 j_2^2 - 15\right)}{\left(j_2^2 + 1\right)^2}, \end{aligned} \tag{5.12}$$

respectively. Here j_1 and j_2 means $j(Y_1)$ and $j(Y_2)$, as given in Eq. (C6), and $\delta_1 \equiv Y_C - Y_1$, $\delta_2 \equiv Y_C - Y_2$.

We note the interesting special cases in which one of the two operators σ or ϵ is close to the base line while the other one is close to the corner. The corresponding results are

$$\mathscr{R}(y_1,\ y_2) \to -5\left(\frac{Y_C}{y_C}\right)^8 y_2\, (y_C - y_1)^{6-(1/8)}\, 2^{-8+(1/8)}\, 3^{1+(1/8)}, \quad y_2 \to 0, \quad y_1 \to y_C \tag{5.13}$$

and

$$\mathscr{R}(y_1,\ y_2) \to 5\left(\frac{Y_C}{y_C}\right)^8 y_1^{2-(1/8)}\, (y_C - y_2)^5\, 2^{-8+(1/8)}\, 3^2, \quad y_1 \to 0, \quad y_2 \to y_C. \tag{5.14}$$

The first one follows from either putting Y_1 close to Y_C in $\mathscr{B}_2$ in Eq. (5.9) or from putting $Y_2 \to 0$ in $\mathscr{C}_1$ in Eq. (5.12) and the second one from either putting $Y_1 \to 0$ in $\mathscr{C}_2$ in Eq. (5.10) or from putting Y_2 close to Y_C in $\mathscr{B}_1$ in Eq. (5.11).

For completeness we mention the special cases of (5.9)–(5.12) in which y_1 and y_2 are both near the base line or both near the corner: putting $y_1 \ll y_C$ in $\mathscr{B}_2$ and $y_C - y_1 \ll y_C$ in $\mathscr{C}_2$ yields

$$\mathscr{R}(y_1,\ y_2) \to -\left(\frac{2}{y_1}\right)^{1/8} \frac{y_2}{y_1^2}, \quad y_2 \ll y_1 \ll y_C \tag{5.15}$$

and

$$\mathscr{R}(y_1,\ y_2) \to 3^{(1/8)+1} \left(\frac{2}{y_C - y_1}\right)^{1/8} \frac{(y_C - y_2)^5}{(y_C - y_1)^6}, \quad y_C - y_2 \ll y_C - y_1 \ll y_C, \tag{5.16}$$

respectively. As expected Eqs. (5.15) and (5.16) reproduce the simple results when the triangle degenerates to the infinitely extended base line and to the infinitely extended wedge, respectively, the point 2 being much closer to the basis and to the corner

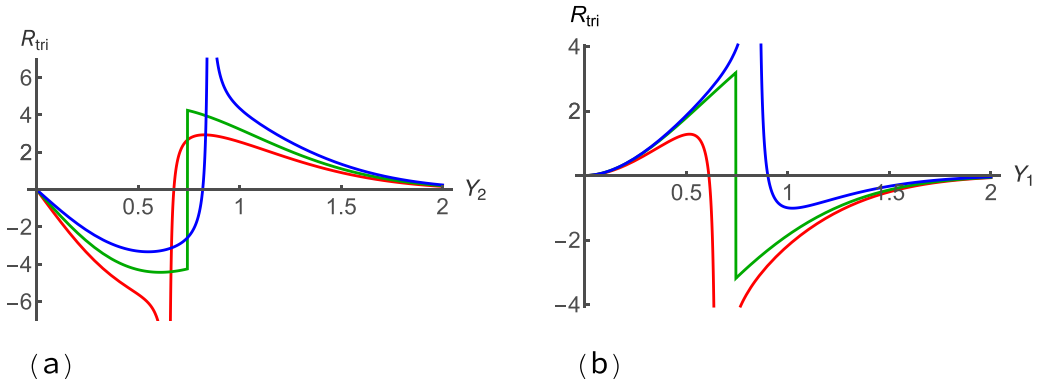


FIG. 3. Dimensionless response function $R_{\rm tri}$ on the vertical midline of the triangle defined in Eq. (5.19) and evaluated by means of (5.20). The red, green, and blue curves in panel (a) show the dependencies of $R_{\rm tri}$ on Y_2 for Y_1 fixed at 0.65, at $Y_0 = 0.743$, and at 0.85. The response $R_{\rm tri}$ of the disorder to the up ordering at $Y_1 = Y_0$ (green curve) is negative and positive at $Y_2 < Y_0$ and $Y_2 > Y_0$ since there the original order is in the up and down direction, respectively. For Y_2 close to Y_0 the Y_2 dependence reflects the asymptotic behavior given in Eq. (5.21) with an upward discontinuity where $R_{\rm tri}$ jumps from $-(2S_0)^{9/8} \equiv -(3^{3/4}2^{2/3})^{9/8} = -4.249$ to $(2S_0)^{9/8}$. Unlike panel (a) in Fig. 2 the Y_2 dependence is not antisymmetric about the discontinuity and near the base line $Y = 0$ and the corner $Y = Y_{\rm C} \equiv 3.196$ of the triangle it attains the behavior determined by Eqs. (5.9) and (5.10). This decreases linearly from zero and approaches zero with the fifth power in the distance from the corner, respectively. For $Y_1 \neq Y_0$ [red and blue curves in panel (a)] the short distance singularity is $\propto |Y_2 - Y_1|^{-1}\,{\rm sgn}(Y_1 - Y_0)$ and the prefactors of the near baseline and corner behaviors depend on Y_1 according to Eqs. (5.9) and (5.10). Panel (b) shows the Y_1 dependence of the up order induced by the disorder imposed at Y_2 for Y_2 fixed at 0.65 (red), at Y_0 (green), and at 0.85 (blue). For $Y_2 = Y_0$ there is a downward discontinuity in the Y_1 dependence and the ratio of the discontinuities in panels (a) and (b) has the universal value of $-4/3$. Both for $Y_2 = Y_0$ and $Y_2 \neq Y_0$ the power law behaviors of Y_1 near the base line and the corner have exponents $2 - (1/8)$ and $6 - (1/8)$, respectively, with Y_2-dependent amplitudes according to Eqs. (5.11) and (5.12). Note the $Y_1 < Y_0$ regions with $\mathrm{R}_{\rm tri} > 0$ and the $Y_1 > Y_0$ regions with $\mathrm{R}_{\rm tri} < 0$, where the magnitude of the order is *enhanced* by the disordering.

of the wedge, respectively, than point 1. These results follow from Eq. (2.4) and its wedge transform. Likewise, for the cases in which point 1 is much closer than point 2 to the basis and the corner one invokes Eqs. (5.11) and (5.12) with $\mathscr{B}_1(Y_2 \to 0)$ and $\mathscr{C}_1(Y_2 \to Y_{\rm C})$, respectively, which yields the expected results

$$\mathscr{R}(y_1,\, y_2) \to -\left(\frac{2}{y_1}\right)^{1/8} \frac{y_1^2}{y_2^3}, \quad y_1 \ll y_2 \ll y_{\rm C} \tag{5.17}$$

and

$$\mathscr{R}(y_1,\, y_2) \to 3^{(1/8)+1} \left(\frac{2}{y_{\rm C} - y_1}\right)^{1/8} \frac{(y_{\rm C} - y_1)^6}{(y_{\rm C} - y_2)^7}, \quad y_{\rm C} - y_1 \ll y_{\rm C} - y_2 \ll y_{\rm C}. \tag{5.18}$$

In Eqs. (5.21) and (5.22) below we discuss the short distance behavior of $\mathscr{R}$ for the cases in which σ or ϵ are located at the point $y = y_0 = 0.2325 \times y_{\rm C}$ of the midline where $\langle\sigma\rangle_{\rm triangle}$ vanishes [19]; see Eq. (C8)ff. This point belongs to the zero line of our triangle that starts and ends at the corners $z_{\rm A}$ and $z_{\rm B}$ and crosses the midline at $z = iy_0$.

Finally we consider the behavior of our response function on the vertical midline of the triangle, $\langle\sigma(x_1 = 0, y_1)\,\epsilon(x_2 = 0, y_2)\rangle^{\rm (cum)}_{\rm triangle} \equiv \mathscr{R}(y_1,\, y_2)$, for *arbitrary* y_2 with y_1 fixed at several values and vice versa. This is shown in panels (a) and (b), respectively, of Fig. 3 in terms of the dimensionless response function $R_{\rm tri}(Y_1,\, Y_2)$ which is defined by

$$\mathscr{R}(y_1,\, y_2) = \left(\frac{Y_{\rm C}}{y_{\rm C}}\right)^{(1/8)+1} R_{\rm tri}(Y_1,\, Y_2), \quad Y = \frac{Y_{\rm C}}{y_{\rm C}}\, y. \tag{5.19}$$

Since the midline of the triangle extends over the interval $0 < y < y_{\rm C}$, the variables Y_1 and Y_2 extend along $0 < Y < Y_{\rm C} \equiv 3.196$; see Eq. (C8). The original order is positive and negative for $Y < Y_0$ and $Y > Y_0$, respectively, with $Y_0 \equiv 0.7432$; see Eq. (5.3). To calculate $R_{\rm tri}$ one uses (5.2) that implies

$$R_{\rm tri}(Y_1,\, Y_2) = S(iY_1)^{1/8}\, S(iY_2)\, \langle\sigma(g_1 = 0,\, j_1)\,\epsilon(g_2 = 0,\, j_2)\rangle^{\rm (cum)}_{-+-}|_{j = j(Y)}, \tag{5.20}$$

where the expressions for the cumulant $\langle\ldots\rangle^{\rm (cum)}_{-+-}$, for $j(Y)$, and for $S(iY)$ are given in Eqs. (4.16), (C6), and (C9), respectively.

Equation (5.20) implies for $Y_1 = Y_0$ and for $Y_2 = Y_0$ the short distance behaviors up to linear order

$$R_{\rm tri}(Y_1 = Y_0,\, Y_2) \;\to\; (2S_0)^{9/8} \times \left[{\rm sgn}(Y_2 - Y_0) \;-\; \frac{S_0}{3}\,|Y_2 - Y_0| + O((Y_2 - Y_0)^2)\right] \tag{5.21}$$

and

$$R_{\rm tri}(Y_1,\ Y_2=Y_0)\to -(2S_0)^{9/8}\times\frac{3}{4}\left[\mathrm{sgn}(Y_1-Y_0)-\frac{S_0}{3}\left(\frac{|Y_1-Y_0|}{8}+3\,(Y_1-Y_0)\right)+O((Y_1-Y_0)^2)\right]. \tag{5.22}$$

Here the number S_0 is given by Eq. (C11) and we used the corresponding behaviors (4.12) and (4.15) in the $-+-$ half plane and the relations (C10). The universal ratio $-4/3$ between the upward and downward discontinuities is clearly visible. The tangents to the left and right of the discontinuities in panels (a) and (b) of Fig. 3 are given by the linear order terms in Eqs. (5.21) and (5.22), respectively. In Appendix A 6 Eq. (5.21) is confirmed by means of the operator-product expansion.

VI. $\mathscr{W}\times\mathscr{W}$ SQUARE WITH VERTICAL BOUNDARIES $-$ AND HORIZONTAL BOUNDARIES $+$

Consider a square with vertical boundaries $-$ and horizontal boundaries $+$ with its center at the origin of the entire $z=x+iy$ plane, which is mirror-symmetric about the coordinate axes, implying for the two-point function $\langle\sigma\,\epsilon\rangle_{\rm SQ}$ for example that

$$\begin{aligned}\langle\sigma(x_1,y_1)\,\epsilon(x_2,y_2)\rangle_{\rm SQ}^{\rm (cum)}&=\langle\sigma(-x_1,y_1)\,\epsilon(-x_2,y_2)\rangle_{\rm SQ}^{\rm (cum)},\\&=\langle\sigma(x_1,-y_1)\,\epsilon(x_2,-y_2)\rangle_{\rm SQ}^{\rm (cum)}.\end{aligned} \tag{6.1}$$

Moreover, mirror imaging about the diagonals interchanges boundary conditions $+\leftrightarrow-$, which turns $\sigma,\ \epsilon$ into $-\sigma,\ \epsilon$. Thus

$$\begin{aligned}[\langle\sigma(x,y)\rangle_{\rm SQ}]|_{x,y\to y,x}=-\langle\sigma(x,y)\rangle_{\rm SQ},\quad [\langle\epsilon(x,y)\rangle_{\rm SQ}]|_{x,y\to y,x}=\langle\epsilon(x,y)\rangle_{\rm SQ},\\ [\langle\sigma(x_1,y_1)\,\epsilon(x_2,y_2)\rangle_{\rm SQ}]|_{x_1,y_1;x_2,y_2\to y_1,x_1;y_2,x_2}=-\langle\sigma(x_1,y_1)\,\epsilon(x_2,y_2)\rangle_{\rm SQ}\end{aligned} \tag{6.2}$$

and, in particular, $\langle\sigma\rangle_{\rm SQ}$ vanishes at the diagonals. The same symmetry relations apply to the two-point cumulants.

Putting either σ or ϵ at the origin, where the two zero-line diagonals intersect, and the other operator close to it, the leading behavior is given by

$$\begin{aligned}\langle\sigma(x_1=0,y_1=0)\,\epsilon(x_2,y_2)\rangle_{\rm SQ}&\to\frac{16}{3}\Lambda^{-(1/8)-2}\,2^{1/4}\times\frac{x_2^2-y_2^2}{\sqrt{x_2^2+y_2^2}},\\ \langle\sigma(x_1,y_1)\,\epsilon(x_2=0,y_2=0)\rangle_{\rm SQ}&\to-\frac{5}{3}\Lambda^{-(1/8)-2}\,2^{1/4}\times\frac{x_1^2-y_1^2}{\sqrt{x_1^2+y_1^2}},\end{aligned} \tag{6.3}$$

which is different from the cases in Secs. III–V. Along the midlines the nonanalyticities are not discontinuities but rather the symmetric cusps

$$\begin{aligned}\langle\sigma(x_1=0,y_1=0)\,\epsilon(x_2,y_2=0)\rangle_{\rm SQ}&\to\tfrac{16}{3}\Lambda^{-(1/8)-2}\,2^{1/4}\ \times x_2\ \mathrm{sgn}(x_2),\\ \langle\sigma(x_1=0,y_1=0)\,\epsilon(x_2=0,y_2)\rangle_{\rm SQ}&\to-\tfrac{16}{3}\Lambda^{-(1/8)-2}\,2^{1/4}\times y_2\ \mathrm{sgn}(y_2)\end{aligned} \tag{6.4}$$

and

$$\begin{aligned}\langle\sigma(x_1,y_1=0)\,\epsilon(x_2=0,y_2=0)\rangle_{\rm SQ}&\to-\tfrac{5}{3}\Lambda^{-(1/8)-2}\,2^{1/4}\times x_1\ \mathrm{sgn}(x_1),\\ \langle\sigma(x_1=0,y_1)\,\epsilon(x_2=0,y_2=0)\rangle_{\rm SQ}&\to\tfrac{5}{3}\Lambda^{-(1/8)-2}\,2^{1/4}\,y_1\times\mathrm{sgn}(y_1).\end{aligned} \tag{6.5}$$

Still qualitative features found in Secs. III–V remain. For example, Eq. (6.5) tells us that the order is strengthend by increasing the disorder at the center of our square.

In the above equations $\Lambda^{-1}=\mathbf{K}(1/\sqrt{2})\,/\mathscr{W}$ with $\mathbf{K}(1/\sqrt{2})=1.854$ the complete elliptic integral. These results apply when the nonvanishing coordinate is much smaller than $\mathscr{W}$. They are consistent with the above symmetry relations and, as discussed in Sec. A 7, they follow via the $\mathscr{a}$, $\mathscr{b}$, and $\mathscr{c}$ terms in the OPE (A1) from the form

$$\langle\sigma(x_1,y_1)\rangle_{\rm SQ}\to-\Lambda^{-(1/8)-2}\,2^{1/4}\,2\big(x_1^2-y_1^2\big)\ =\ -\Lambda^{-(1/8)-2}\,2^{1/4}\,\big(z_1^2+\bar z_1^2\big) \tag{6.6}$$

of the one-point function near the center, which is derived in Appendix D. Equations (6.3)–(6.5) apply not only to the two-point function but also to the cumulant $\langle\sigma\,\epsilon\rangle_{\rm SQ}^{\rm (cum)}$ since their difference,

$$\langle\sigma(x_1,y_1)\rangle_{\rm SQ}\times\langle\epsilon(x_2,y_2)\rangle_{\rm SQ}\to-\tfrac{10}{3}\Lambda^{-(1/8)-3}\,2^{1/4}\,\big(x_1^2-y_1^2\big), \tag{6.7}$$

is smaller by a factor x/Λ or y/Λ. Equation (6.7) arises from (6.6) and the form $\langle\epsilon(x_2,y_2)\rangle_{\rm SQ}\to(5/3)\,\Lambda^{-1}$ of the energy density profile near the center.

VII. SUMMARY AND CONCLUDING REMARKS

We consider the two-dimensional critical Ising model with mixed boundary conditions and ask how local ordering imposed at point $\mathbf{r}_1$ affects the disorder at another point $\mathbf{r}_2$ and vice versa. The answer is contained in the universal cumulant response function $\langle\sigma(\mathbf{r}_1)\,\epsilon(\mathbf{r}_2)\rangle^{\rm (cum)}$, where σ and ϵ are the

density operators of the order parameter and energy. Making use of the OPE for $\sigma \times \epsilon$ and exact results, we study the response function of systems in the upper half plane with (1) a uniform boundary $+$ of fixed up spins, (2) a mixed boundary $+-$ of fixed up and down spins on the negative and positive boundary line, respectively, and (3) a $-+-$ boundary consisting of a finite segment of up spins between two semi-infinite segments of down spins. We also consider two finite systems: (4) an equilateral triangle with up spins on one edge, the horizontal base line of the triangle, and down spins on the other two edges, and (5) a square with up spins on the horizontal edges and down spins on the vertical edges. The mixed boundaries in (2)–(5) generate zero lines along which the order-parameter profile $\langle\sigma\rangle$ vanishes.

Figures 2 and 3 show the remarkable behavior of the response function, associated with zero lines, as $\mathbf{r}_1$ and $\mathbf{r}_2$ vary along a line parallel to the boundary of the half plane (2) and along the vertical midline of the triangle (4).

The response function $\langle\sigma\epsilon\rangle^{(\mathrm{cum})}$ for (2) is known exactly [3] and transforming it conformally leads to exact expressions for (3) and (4). Despite this, some of the interesting implications seem to have been overlooked. We have shown the utility of the OPE in analyzing the behavior for small $|\mathbf{r}_{12}|$, an approach which is not limited to the Ising model but applicable to a broader class of systems.

The OPEs in Eqs. (1.1) and (1.3) imply that, in *leading* order, $\langle\sigma\epsilon\rangle^{(\mathrm{cum})}$ at short distances $|\mathbf{r}_{12}|$ depends on local properties of the order-parameter density $\langle\sigma\rangle$. This is in contrast to the correlation functions $\langle\sigma\sigma\rangle^{(\mathrm{cum})}$ and $\langle\epsilon\epsilon\rangle^{(\mathrm{cum})}$, where the dependence on the corresponding symmetry-allowed profiles $\langle\epsilon\rangle$ or $\langle T\rangle$ only appears in higher order [12]. For nonvanishing $\langle\sigma\rangle$, the leading singularity of $\langle\sigma\epsilon\rangle^{(\mathrm{cum})}$ has the form of a power law divergence with magnitude proportional to $\langle\sigma\rangle$ but with the opposite sign; see Eq. (2.2) and panel (i) of Fig. 1. On placing one of the two operators on a zero line of $\langle\sigma\rangle$ and crossing the line with the other operator, the leading short-distance singularity is milder, having the form of a discontinuity, a cusp, etc., depending on the lowest nonvanishing derivative of $\langle\sigma\rangle$. For systems (2), (3), and (4), the singularity is a discontinuity such as in panels (ii) and (iii) of Fig. 1, while at the center of the square (5), where the first derivatives vanish, it is a cusp. The ratio of the two discontinuities, when one of the two operators σ or ϵ is placed on a point of the zero line while the other one crosses it, is a universal number. All this is a consequence of the operator-product expansion (1.3) and its extension to higher order in Appendix A.

We also analyze the behavior of the response function as one of the two operators σ or ϵ approaches a flat boundary or a corner, making use of the boundary-operator expansion or corner-operator expansion, respectively. As the operator σ approaches the upper vertex or corner of the equilateral triangle along the midline between the sides of fixed down spins, the response function decays with power law exponents $47/8$ and for ϵ the exponent is 5, with an amplitude that depends on the position of the other operator. It would be interesting to compare these predictions with simulations.

ACKNOWLEDGMENT

I thank T. W. Burkhardt for many useful discussions.

DATA AVAILABILITY

No data were created or analyzed in this study.

APPENDIX A: OPERATOR EXPANSION OF THE PRODUCT $\sigma \times \epsilon$ UP TO FOURTH ORDER

Unlike the Cartesian language used in Eqs. (1.3) for the OPE in low order, for higher order it is advantageous to use the complex notation; see Ref. [7]. Extending the OPE (1.3) by two more orders the result can be written as

$$\sigma(z_1,\bar z_1)\epsilon(z_1+z_{21},\bar z_1+\bar z_{21}) \to -\frac{1}{2}\frac{1}{|z_{21}|}\times\Big[1+\mathscr{a}(z_{21}L_{-1}+\bar z_{21}\bar L_{-1})+\mathscr{b}\big(z_{21}^2L_{-1}^2+\bar z_{21}^2\bar L_{-1}^2\big)+\mathscr{c}|z_{21}|^2L_{-1}\bar L_{-1}$$
$$+\alpha\big(z_{21}^3L_{-3}+\bar z_{21}^3\bar L_{-3}\big)+\beta\big(z_{21}^3L_{-1}^3+\bar z_{21}^3\bar L_{-1}^3\big)+\gamma\big(z_{21}^2\bar z_{21}L_{-1}^2\bar L_{-1}+\bar z_{21}^2z_{21}\bar L_{-1}^2L_{-1}\big)\Big]\times\sigma(z_1,\bar z_1), \tag{A1}$$

where

$$\mathscr{a}=4,\quad \mathscr{b}=\tfrac{8}{3},\quad \mathscr{c}=16 \tag{A2}$$

and

$$\alpha=-\tfrac{4}{7},\quad \beta=\tfrac{32}{21},\quad \gamma=\tfrac{32}{3}. \tag{A3}$$

Since $\sigma\times\epsilon$ is odd on reversing all Ising spins the expansion (A1) is in terms of σ and its descendants. These arise from it by repeatedly applying the operations [7,20]

$$L_{-p}\,\Sigma(z_1,\bar z_1)\equiv\int_{\mathscr{C}_{z_1}}\frac{\mathrm{d}z}{2\pi i}(z-z_1)^{-p+1}T(z)\,\Sigma(z_1,\bar z_1),$$
$$\bar L_{-p}\,\Sigma(z_1,\bar z_1)\equiv\int_{\mathscr{C}_{\bar z_1}}\frac{\mathrm{d}\bar z}{2\pi i}(\bar z-\bar z_1)^{-p+1}\bar T(\bar z)\,\Sigma(z_1,\bar z_1), \tag{A4}$$

with $p=1,2,3,\ldots$. Here $\mathscr{C}_{z_1}$ and $\mathscr{C}_{\bar z_1}$ are closed integration paths enclosing counterclockwise the points z_1 and $\bar z_1$, respectively. In particular, $L_{-1}\,\Sigma(z_1,\bar z_1)=\partial_{z_1}\Sigma(z_1,\bar z_1)$. Consecutive operations do not in general commute, but follow the Virasoro algebra

[7], since the integration path of the operation to the right is nested inside the integration path of the one to the left. Due to the degeneracy of σ on level 2 in the Ising model, $L_{-2}\,\sigma = (4/3)L_{-1}^2\,\sigma$, and, choosing $L_{-1}^2\,\sigma$, the operator $L_{-2}\,\sigma$ does not appear in (A1). Moreover, $L_{-2}\,L_{-1}\,\sigma$ does not appear since it can be expressed via the Virasoro algebra [7] in terms of $L_{-1}L_{-2}\,\sigma$ and $L_{-3}\,\sigma$, i.e., in terms of $L_{-1}^3\,\sigma$ and $L_{-3}\,\sigma$.

In the following the second, third, and fourth order terms in Eq. (A1) will often be addressed as the first, second, and third corrections.

1. Derivation by comparing with the four-point function in the bulk

The operator form in (A1) is consistent with the general expression of the OPE for two primary operators given in Ref. [7] and the prefactors that are specific for the product $\sigma \times \epsilon$ in the Ising model can be obtained by comparing with the bulk four point function $\langle\sigma(1)\,\epsilon(2)\,\sigma(3)\,\epsilon(4)\rangle$ taken from Eq. (32) of Ref. [21]. In particular, to obtain the values in (A3), we expand the four point function with $z_1 = 0$ and $z_{21} = 1$ for large $|z_3|$, $|z_4|$ and find in the order of the third correction the result

$$\begin{aligned}\langle\sigma(0,0)\,\epsilon(1,0)\,\sigma(z_3,\bar z_3)\,\epsilon(z_4,\bar z_4)\rangle_{\rm bulk}|_{\rm 3rd\,corr} = -\tfrac{1}{16}\Theta\,{\rm Re}\big[&-7z_3^{-3} + 32z_4^{-3} - 16z_3^{-1}z_4^{-2} - 4z_3^{-2}z_4^{-1} + 15z_3^{-2}\bar z_3^{-1}\\ &+ 64z_4^{-2}\bar z_4^{-1} - 48z_3^{-1}\bar z_4^{-2} - 20z_3^{-2}\bar z_4^{-1} + 24|z_3|^{-2}z_4^{-1} - 32|z_4|^{-2}z_3^{-1}\big],\end{aligned} \tag{A5}$$

where [11]

$$\Theta = \langle\sigma(z_3,\bar z_3)\epsilon(z_4,\bar z_4)\sigma(0,0)\rangle_{\rm bulk} \equiv -\tfrac{1}{2}|z_3|^{3/4}|z_4|^{-1}|z_3 - z_4|^{-1}. \tag{A6}$$

Due to the general bulk relation [22]

$$2\,{\rm Re}\big\langle\sigma(z_3,\bar z_3)\,\epsilon(z_4,\bar z_4) \times (-1/2)\big(\big[\alpha L_{-3} + \beta L_{-1}^3 + \gamma L_{-1}^2\bar L_{-1}\big]\sigma(z_1,\bar z_1)\big)\big\rangle_{\rm bulk}\big|_{z_1=0} = \Theta\,{\rm Re}(\mathscr{T}), \tag{A7}$$

with

$$\begin{aligned}\mathscr{T} = &\frac{\alpha}{4}\big(z_3^{-3} - 6z_4^{-3} + 2z_3^{-1}z_4^{-2} + 2z_3^{-2}z_4^{-1}\big)\\ &+ \frac{3\beta}{512}\big(65z_3^{-3} - 320z_4^{-3} + 144z_3^{-1}z_4^{-2} + 60z_3^{-2}z_4^{-1}\big)\\ &+ \frac{3\gamma}{512}\big(-15z_3^{-2}\bar z_3^{-1} - 64z_4^{-2}\bar z_4^{-1} + 20z_3^{-2}\bar z_4^{-1} + 48z_4^{-2}\bar z_3^{-1} - 24|z_3|^{-2}z_4^{-1} + 32|z_4|^{-2}z_3^{-1}\big),\end{aligned} \tag{A8}$$

the OPE (A1) is consistent with the result (A5), (A6) of the four point function if α, β, γ take the values given in Eq. (A3).

2. Checking against the three-point function

Expanding the three-point function [11] in complex notation,

$$\langle\sigma(0,0)\,\epsilon(z_2 = x, \bar z_2 = x)\sigma(z_3,\bar z_3)\rangle_{\rm bulk} \equiv -\frac{1}{2}\,\frac{(z_3\bar z_3)^{3/8}}{|x|(z_3 - x)^{1/2}(\bar z_3 - x)^{1/2}}, \tag{A9}$$

up to order $x^3/|x|$ yields

$$\langle\sigma(0,0)\,\epsilon(x,x)\,\sigma(z_3,\bar z_3)\rangle_{\rm bulk} \to -\frac{1}{2}\,\frac{1}{|x||z_3|^{1/4}} \times \left\{1 + x\,{\rm Re}z_3^{-1} + \frac{x^2}{4}\big(3\,{\rm Re}z_3^{-2} + |z_3|^{-2}\big) + \frac{x^3}{8}\big(5\,{\rm Re}z_3^{-3} + 3\,{\rm Re}z_3^{-1}\bar z_3^{-2}\big)\right\}. \tag{A10}$$

First we confirm that the term $\propto x^2/|x|$ in (A10) is reproduced by multiplying the sum of the $\mathscr{b}$ and $\mathscr{c}$ terms in (A1) with $\sigma(z_3,\bar z_3)$, taking the bulk average, and finally putting $z_{21} = x$ and $z_1 = 0$. Using that $\langle\sigma(z_1,\bar z_1)\,\sigma(z_3,\bar z_3)\rangle_{\rm bulk} = (z_1 - z_3)^{-1/8}(\bar z_1 - \bar z_3)^{-1/8}$ one realizes that the first and second term in the bracket that multiplies $x^2/4$ in (A10) follows from the $\mathscr{b}$ and $\mathscr{c}$ term, respectively.

Next consider the term $\propto x^3/|x|$, for which the OPE (A1) predicts

$$\begin{aligned}&\langle\sigma(0,0)\,\epsilon(x,x)\,\sigma(z_3,\bar z_3)\rangle_{\rm bulk}|_{\rm 3rd\,corr} = -\frac{1}{2}\,\frac{x^3}{|x|} \times \mathscr{S},\\ &\mathscr{S} \equiv 2\,{\rm Re}\big\langle\sigma(z_3,\bar z_3)\big(\big[\alpha L_{-3} + \beta L_{-1}^3 + \gamma L_{-1}^2\bar L_{-1}\big]\sigma(z_1,\bar z_1)\big)\big\rangle_{\rm bulk}\big|_{z_1=0}.\end{aligned} \tag{A11}$$

Using the relationship

$$\mathscr{S} = 2\,{\rm Re}\left[\left(\frac{\alpha}{4} + \frac{153}{512}\beta\right)z_3^{-3} + \frac{9\gamma}{512}z_3^{-2}\bar z_3^{-1}\right]|z_3|^{-1/4}, \tag{A12}$$

see Eq. (B1) in the paper of Ref. [22], together with the prefactors in (A3), one verifies that the prediction (A11) reproduces the term $\propto x^3/|x|$ in Eq. (A10).

3. Applying the OPE in the upper half plane with uniform boundary condition +

A simple check of the OPE in (A1) in the presence of a boundary is provided by averaging it in the upper half plane with a *uniform* boundary condition + and comparing the result with the exact result of $\langle\sigma\epsilon\rangle_+$ in Eq. (2.1). While the expansion about z_1 in direction $z_{21}=x_{21}$ contains only even powers, the one in direction $z_{21}=iy_{21}$ contains both even and odd powers in y_{21}. In the latter case Eq. (2.1) yields

$$\langle\sigma(z_1,\bar z_1)\,\epsilon(z_1+iy_{21},\bar z_1-iy_{21})\rangle_+ \to -\frac{1}{2|y_{21}|}\left(1-\frac{1}{2}Y+\frac{3}{4}Y^2-\frac{7}{8}Y^3+\cdots\right)\langle\sigma(z_1,\bar z_1)\rangle_+, \tag{A13}$$

where $Y\equiv y_{21}/y_1$.

To compare with the OPE, we start with the Y^2 term in (A13) which on using the expression $\langle\sigma(z_1,\bar z_1)\rangle_+=(4i/(z_1-\bar z_1))^{1/8}$ is reproduced by the sum of the $\mathscr{b}$ and $\mathscr{c}$ terms in (A1). Here the contribution of the $\mathscr{b}$ term is by a factor 3 smaller than the contribution of the $\mathscr{c}$ term.

Now consider the Y^3 term in (A13) to be reproduced by the contributions from the α, β, and γ terms in the OPE (A1). First we evaluate $\langle L_{-3}\sigma(z_1,\bar z_1)\rangle_+$. For later use we note the expressions for the more general case of the +− boundary condition where

$$\langle L_{-3}\,\sigma(z_1,\bar z_1)\rangle_{+-}=\int_{\mathscr{C}_{z_1}}\frac{\mathrm{d}z}{2\pi i}(z-z_1)^{-2}\langle T(z)\,\sigma(z_1,\bar z_1)\rangle_{+-}, \tag{A14}$$

with [3]

$$\begin{aligned}\langle T(z)\,\sigma(z_1,\bar z_1)\rangle_{+-}&=[(1)+(2)+(3)+(4)+(5)+(6)]\langle\sigma(z_1,\bar z_1)\rangle_{+-}^{(\zeta)}|_{\zeta=0},\\ (1)&=\frac{1/16}{(z-z_1)^2},\quad (2)=\frac{1}{z-z_1}\partial_{z_1},\quad (3)=\frac{1/16}{(z-\bar z_1)^2},\quad (4)=\frac{1}{z-\bar z_1}\partial_{\bar z_1},\\ (5)&=\langle T(z)\rangle_{+-},\quad (6)=\frac{1}{z-\zeta}\partial_\zeta.\end{aligned} \tag{A15}$$

Here ζ is the switching point on the boundary. Note that the terms (1) and (2) do not contribute to the integral in (A14). For the present uniform + boundary the average of σ is $\langle\sigma(z_1,\bar z_1)\rangle_+=(4i/(z_1-\bar z_1))^{1/8}$ and the terms (5) and (6) are absent. Expanding (3) and (4) about z_1 to first order in $z-z_1$ yields

$$\langle L_{-3}\,\sigma(z_1,\bar z_1)\rangle_+=-\frac{1}{4}\frac{1}{(z_1-\bar z_1)^3}\langle\sigma(z_1,\bar z_1)\rangle_+. \tag{A16}$$

The two remaining third-order terms in (A1) are easily evaluated since $L_{-1}=\partial_{z_1}$ and $\bar L_{-1}=\partial_{\bar z_1}$ and one finds

$$\left\langle\left(L_{-3},\,L_{-1}^3,\,L_{-1}^2\bar L_{-1}\right)\sigma(z_1,\bar z_1)\right\rangle_+=\left(-\frac{1}{4},\,-\frac{153}{512},\,\frac{153}{512}\right)\times\frac{i}{8y_1^3}\langle\sigma(z_1,\bar z_1)\rangle_+, \tag{A17}$$

which inserted in (A1) for $z_{21}=iy_{21}$ yields

$$\langle\sigma\epsilon\rangle_+|_{\propto Y^3}=-\frac{1}{2|y_{21}|}\,\frac{y_{21}^3}{8y_1^3}\times 2\left[-\frac{1}{4}\alpha-\frac{153}{512}(\beta+\gamma)\right]\langle\sigma(z_1,\bar z_1)\rangle_+. \tag{A18}$$

Substituting the values (A3), the square bracket equals $-7/2$ and the rhs of (A17) indeed reproduces the Y^3 term in Eq. (A13).

4. Applying the OPE in the upper half plane with mixed boundary condition +−

a. Case $x_1=0$

Here we show that the OPE (A1) reproduces not only the leading but also the next-to-leading behaviors of $\langle\sigma(x_1=0,y_1=y_0)\,\epsilon(x_2,y_2=y_0)\rangle_{+-}$ near $x_2=0$, which are displayed in Eq. (3.3). In the complex notation of the OPE (A1) we have

$$z_1=iy_0,\quad z_2=iy_0+x_2,\quad \text{so that } z_{21}=x_2 \tag{A19}$$

and we shall need the expressions [3]

$$\begin{aligned}\langle\sigma(z_1,\bar z_1)\rangle_{+-}&=-\left(\frac{4i}{z_1-\bar z_1}\right)^{1/8}\times\frac{1}{(z_1\bar z_1)^{1/2}}\times\frac{z_1+\bar z_1}{2},\\ \partial_\zeta\langle\sigma(z_1,\bar z_1)\rangle_{+-}^{(\zeta)}|_{\zeta=0}&=2^{1/8}\left(\frac{2i}{z_1-\bar z_1}\right)^{1/8-2}\times\frac{1}{(z_1\bar z_1)^{3/2}}.\end{aligned} \tag{A20}$$

Calculating $\langle L_{-3}\,\sigma\rangle_{+-}$ along Eqs. (A14) and (A15) the terms (3) and (5) do not contribute since they are proportional to $\langle\sigma\rangle_{+-}$ which vanishes for $x_1=0$ so that only the terms (4) and (6) survive. Due to $(\partial_{\bar z_1},\partial_\zeta)\langle\sigma(z_1,\bar z_1)\rangle_{+-}=(-1/2,1)(2/y_0)^{1/8}y_0^{-1}$ for

our $z_1 = iy_0$, expanding the prefactors in (4) and (6) to first order in $z - z_1$ yields

$$\langle L_{-3}\,\sigma(z_1,\bar z_1)\rangle_{+-}|_{z_1=iy_0} = \frac{7}{8}\,\frac{1}{y_0^3}\left(\frac{2}{y_0}\right)^{1/8}. \tag{A21}$$

For the averages of the other two descendants of σ one finds

$$\left\langle\left(L_{-1}^3,\ L_{-1}^2\bar L_{-1}\right)\sigma(z_1,\bar z_1)\right\rangle_{+-}\Big|_{z_1=iy_0} = \frac{3}{512}\,(217,\ 13)\frac{1}{y_0^3}\left(\frac{2}{y_0}\right)^{1/8}. \tag{A22}$$

Here one uses $L_{-1} = \partial_{z_1}$, $\bar L_{-1} = \partial_{\bar z_1}$, and the differentiations are simplified since for a nonvanishing result for $z_1 = iy_0$ the last factor in the upper equation (A20) must always be differentiated. Substituting (A21) and (A22) in (A1) yields

$$\langle\sigma\epsilon\rangle_{+-}|_{z_1=iy_0,\,z_2=iy_0+x_2}|_{\text{3rd corr}} = -\frac{1}{2}\,\frac{1}{|x_2|}\left(\frac{x_2}{y_0}\right)^3\left(\frac{2}{y_0}\right)^{1/8} \times 2\left[\frac{7}{8}\alpha + \frac{3\times 217}{512}\beta + \frac{39}{512}\gamma\right]. \tag{A23}$$

Inserting (A3) the square bracket takes the value 9/4 and (A23) reproduces the next-to-leading order term for small $|x_2|$ in (3.3).

b. Case $x_2 = 0$

Here we have

$$z_1 = iy_0 + x_1, \quad z_2 = iy_0, \quad \text{so that } z_{21} = -x_1. \tag{A24}$$

When correspondingly inserting $z_1 = iy_0 + x_1$, $z_{21} = -x_1$ in the OPE (A1) and taking the average $\langle\,\rangle_{+-}$ the RHS displays an x_1 dependence proportional to $(1/|x_1|)\,[x_1,\ x_1^3,\ x_1^5,$ etc.], consistent with the exact result of the two-point function $\langle\sigma\,\epsilon\rangle_{+-}$ in Eq. (3.4). The reason is that even powers of $z_{21} = \bar z_{21} = -x_1$ are accompanied by averages of σ descendants that are odd in x_1 and vice versa. The leading order contribution to $\langle\sigma\,\epsilon\rangle_{+-}$ comes from the first two terms in the square bracket in (A1) which yields

$$\langle\sigma(iy_0 + x_1, -iy_0 + x_1)\,\epsilon(iy_0, -iy_0)\rangle_{+-} \to -\frac{1}{2|x_1|}\left(\frac{2}{y_0}\right)^{1/8}\frac{x_1}{y_0}\,(-1 + \mathscr{a}) \tag{A25}$$

with $\mathscr{a} = 4$ from (A2). This reproduces the leading behavior of the two-point function given in Eq. (3.4).

5. OPE in the upper half plane with a $-+-$ boundary

Now we apply the OPE (A1) about the point $g_1 = 0,\ j_1 = 1$ in the upper half h plane with a $-+-$ boundary where $\langle\sigma\rangle_{-+-}$ vanishes and show that it reproduces the expansion (4.10). Here $h_1 = i$ and $h_{21} = g_2 + i(j_2 - 1)$.

The contribution to $\langle\sigma\,\epsilon\rangle_{-+-}$ in (4.10) from the second term in its curly bracket follows from the $\mathscr{b}$ and $\mathscr{c}$ terms in (A1). For the evaluation it helps to rewrite (4.7) in the form

$$\langle\sigma(h_1,\bar h_1)\rangle_{-+-} = (1 - |h_1|^2) \times \mathscr{D}, \quad \mathscr{D} \equiv \left(\frac{4i}{h_1 - \bar h_1}\right)^{1/8}\left(1 - h_1^2\right)^{-1/2}\left(1 - \bar h_1^2\right)^{-1/2} \tag{A26}$$

and to observe that [23]

$$\begin{aligned}\left\langle L_{-1}^2\sigma\right\rangle_{-+-}\Big|_{h_1=i} &\equiv \partial_{h_1}^2\langle\sigma\rangle_{-+-}\Big|_{h_1=i} = -2\bar h_1\partial_{h_1}\mathscr{D}\Big|_{h_1=i} = -2^{1/8}\,9/16,\\ \langle L_{-1}\bar L_{-1}\sigma\rangle_{-+-}\Big|_{h_1=i} &\equiv \partial_{h_1}\partial_{\bar h_1}\langle\sigma\rangle_{-+-}\Big|_{h_1=i}\\ &= -\left[1 + \left(h_1\partial_{h_1} + \bar h_1\partial_{\bar h_1}\right)\right]\mathscr{D}\Big|_{h_1=i} = 2^{1/8}/16.\end{aligned} \tag{A27}$$

Together with the above form of h_{21} and the coefficients (A2) the OPE (A1) in the h plane then leads to the desired contribution in (4.10).

The contribution to $\langle\sigma\,\epsilon\rangle_{-+-}$ in (4.10) from the third term in its curly bracket follows from the α, β, and γ terms in the OPE (A1) and is reproduced by using the results

$$\left\langle\left(\alpha L_{-3},\ \beta L_{-1}^3,\ \gamma L_{-1}^2\bar L_{-1}\right)\sigma(h_1,\ \bar h_1)\right\rangle_{-+-}\Big|_{h_1=i} = -\,2^{1/8}\,\frac{i}{16\times 7}\,(-40,\ 89,\ 49). \tag{A28}$$

Finally consider the OPE about the point $g_2 = 0,\ j_2 = 1$, i.e., $h_2 = i$. Here (A1) yields

$$\langle\sigma(g_1 = 0,\, j_1)\,\epsilon(g_2 = 0,\, j_2 = 1)\rangle_{-+-} \to -\frac{2^{(1/8)+1}}{4|j_1 - 1|}\left[(j_1 - 1)\,(-1 + \mathscr{a}) + (j_1 - 1)^2\left(\frac{5}{8} - \frac{5}{4}\mathscr{a} + \frac{9}{8}\mathscr{b} + \frac{1}{16}\mathscr{c}\right)\right], \tag{A29}$$

which on inserting the values given in (A2) reproduces (4.14).

6. OPE in the triangle

Here we derive the result (5.21) within the OPE, showing how it follows from the $\mathscr{a}$, $\mathscr{b}$, and $\mathscr{c}$ terms. For the present purpose let us write Eq. (A1) in the form

$$\langle\sigma(z_1=iy_0,\bar z_1)\,\epsilon(z_2=z_1+z_{21},\bar z_2)\rangle^{(\mathrm{cum})}_{\mathrm{triangle}} \to \left(\frac{Y_C}{y_C}\right)^{(1/8)+1}\left(-\frac{1}{2|Z_{21}|}\right)\left[\mathscr{a}(Z_{21}A+\mathrm{c.c.})+\mathscr{b}\left(Z_{21}^2B+\mathrm{c.c.}\right)+\mathscr{c}|Z_{21}|^2C\right], \tag{A30}$$

where

$$(A,B,C)=\left(\partial_{Z_1},\ \partial_{Z_1}^2,\ \partial_{Z_1}\partial_{\bar Z_1}\right)\times\left(S(Z_1)S(\bar Z_1)\right)^{1/16}\langle\sigma(h_1,\bar h_1)\rangle_{-+-}|_{Z_1=iY_0}. \tag{A31}$$

Expressing everything in terms of h via $\partial_{Z_1}=S(Z_1)\partial_{h_1}$ one finds

$$\begin{aligned}
A &= |S|^{1/8}S\left(\partial_{h_1}\langle\sigma\rangle_{-+-}\right)\big|_{h_1=i} = S_0^{(1/8)+1}\,2^{(1/8)-1}\,i,\\
B &= \bar S^{1/16}\left[\tfrac{9}{8}S^{(1/16)+1}\left(\partial_{h_1}S\right)\left(\partial_{h_1}\langle\sigma\rangle_{-+-}\right)+S^{(1/16)+2}\left(\partial_{h_1}^2\langle\sigma\rangle_{-+-}\right)\right]\big|_{h_1=i}\\
&= -S_0^{(1/8)+2}\,2^{(1/8)-1}\,\tfrac{3}{8},\\
C &= \left[\tfrac{1}{16}\left(|S|^{1/8}\bar S\left(\partial_{h_1}S\right)\left(\partial_{\bar h_1}\langle\sigma\rangle_{-+-}\right)+\mathrm{c.c.}\right)+|S|^{(1/8)+2}\left(\partial_{h_1}\partial_{\bar h_1}\langle\sigma\rangle_{-+-}\right)\right]\big|_{h_1=i}\\
&= S_0^{(1/8)+2}\,2^{(1/8)-1}\,\tfrac{1}{24}.
\end{aligned} \tag{A32}$$

Here in the last steps we use the expressions (C5) for S and [23], (A26), (A27) for the h derivatives of $\langle\sigma\rangle_{-+-}$. Substituting A,B,C from (A32) and $\mathscr{a},\mathscr{b},\mathscr{c}$ from (A2) in (A30) and putting $Z_{21}=i(Y-Y_0)$ one arrives at the small-distance expression (5.21).

7. OPE in the square

Here we address the leading short distance behavior of the two-point functions $\langle\sigma\epsilon\rangle_{\mathrm{SQ}}$ in the square of Sec. VI with one of the operators located in the square's center. Their forms are given in Eqs. (6.3)–(6.5) and are derived from the order parameter profile (6.6) using the OPE (A1). While for σ in the center only the $\mathscr{b}$ term contributes, the results for ϵ in the center follow from the three terms 1, $\propto\mathscr{a}$, and $\propto\mathscr{b}$ in the square bracket of Eq. (A1) yielding

$$\langle\sigma(z_1,\bar z_1)\,\epsilon(0,0)\rangle_{\mathrm{SQ}}/\langle\sigma(z_1,\bar z_1)\rangle_{\mathrm{SQ}} \to -\frac{1}{2|z_1|}\,[1-2\mathscr{a}+2\mathscr{b}]. \tag{A33}$$

This leads to the second equation in (6.3).

APPENDIX B: CUMULANTS WITH THE STRESS TENSOR AND NEAR-BOUNDARY BEHAVIOR

Cumulants with the stress tensor follow from the conformal Ward identity. For the half plane with $+-$ boundary condition, see Eq. (2.4) in Ref. [3] which is reproduced in the present Eq. (A15). We are interested in the cumulants $\langle T\,\phi\rangle^{(\mathrm{cum})}$ with $\phi=\sigma$ or ϵ. Besides their importance for the OPE as described in Appendix A, via the BOE [16] they describe the near boundary behavior of the response function $\langle\sigma\epsilon\rangle_{+-}$.

The profiles $\langle\phi\rangle$ and their derivatives with respect to the switch point that are needed for the Ward identity can be taken from Eq. (4.1) in Ref. [3] and from Eqs. (3.28) in Ref. [5], respectively. The results can be written as

$$\langle T(z)\,\sigma(x_1,y_1)\rangle^{(\mathrm{cum})}_{+-} = -\left(\frac{4i}{z_1-\bar z_1}\right)^{1/8}\frac{1}{16}\times\left[\left(\frac{1}{(z-z_1)^2}+\frac{1}{(z-\bar z_1)^2}\right)\frac{z_1+\bar z_1}{2|z_1|}+\frac{1}{z-z_1}P+\frac{1}{z-\bar z_1}\bar P+\frac{4}{z}\frac{(z_1-\bar z_1)^2}{|z_1|^3}\right], \tag{B1}$$

where

$$P\equiv\frac{1}{z_1-\bar z_1}\,\frac{3z_1^2-9|z_1|^2+4\bar z_1^2}{z_1|z_1|} \tag{B2}$$

and

$$\langle T(z)\,\epsilon(x_2,y_2)\rangle^{(\mathrm{cum})}_{+-} = \left\{\left(\frac{1}{(z-z_2)^2}+\frac{1}{(z-\bar z_2)^2}\right)\frac{1}{2i}\left[\frac{1}{z_2-\bar z_2}+\frac{1}{\bar z_2}-\frac{1}{z_2}\right]+\frac{1}{z-z_2}Q+\frac{1}{z-\bar z_2}\bar Q-\frac{1}{zi}\left(\frac{1}{z_2^2}-\frac{1}{\bar z_2^2}\right)\right\}, \tag{B3}$$

where

$$Q \equiv \frac{1}{i}\left(\frac{1}{z_2^2} - \frac{1}{(z_2 - \bar{z}_2)^2}\right). \tag{B4}$$

We have checked the relations

$$\langle \sigma(x_1, y_1)\, \epsilon(x_2, y_2)\rangle_{+-}^{(\mathrm{cum})} \to 4\, y_2 \langle \sigma(x_1, y_1)\, T(x_2)\rangle_{+-}^{(\mathrm{cum})}, \quad y_2 \to 0 \tag{B5}$$

and

$$\langle \sigma(x_1, y_1)\, \epsilon(x_2, y_2)\rangle_{+-}^{(\mathrm{cum})} \to (-2^{1/8}, 2^{1/8})\, y_1^{2-(1/8)} \langle T(x_1)\epsilon(x_2, y_2)\,\rangle_{+-}^{(\mathrm{cum})}, \quad y_1 \to 0 \tag{B6}$$

for $(x_1 < 0, x_1 > 0)$, that are implied by the BOE explained in Ref. [16].

As a simple example consider the special case of (B1),

$$\langle T(z)\, \sigma(x_1 = 0, y_1 = y_0)\rangle_{+-} = \left(\frac{2}{y_0}\right)^{1/8} \frac{y_0}{z\left(z^2 + y_0^2\right)} \tag{B7}$$

and its relation to the response function

$$\langle \sigma(x_1 = 0, y_1 = y_0)\, \epsilon(x_2, y_2)\rangle_{+-} \equiv \left(\frac{2}{y_0}\right)^{1/8} \frac{4 y_0 x_2 y_2}{|z_2|^2 \left|z_2^2 + y_0^2\right|}. \tag{B8}$$

Equation (B8) follows from Eq. (4.3) in Ref. [3] or from (3.6), (3.7) for $z_1 = i y_0$ for which $A = 0$ and $B + C = -8 y_0^2 y_2^2 x_2$. For $y_2 \to 0$ the RHS of (B8) tends to $(2/y_0)^{1/8} 4 y_0 y_2/[x_2(x_2^2 + y_0^2)]$, which on using (B7) is indeed reproduced by the BOE predicting $4 y_2 \langle T(x_2)\sigma(x_1 = 0, y_1 = y_0\rangle_{+-}$ for the LHS of (B8); see Ref. [16].

The relations (B5) and (B6) imply in particular that the cumulants (B1) and (B3) must be real if $z \to x$ becomes real. Moreover, for $z = x$, $\langle T\sigma\rangle_{+-}^{(\mathrm{cum})}$ in (B1) must be odd in x when $x_1 = 0$ and $\langle T\epsilon\rangle_{+-}^{(\mathrm{cum})}$ in (B3) be even in x when $x_2 = 0$ as it follows from the antisymmetry of $\langle \sigma\epsilon\rangle_{+-}^{(\mathrm{cum})}$ given in (3.1).

Next we discuss the cumulants $\langle T(h)\, \phi(g_1, j_1)\rangle_{-+-}^{(\mathrm{cum})}$ in the $-+-$ plane. By means of the Moebius mapping (4.2) and the usual transformation formula one finds, e.g., in the case of $\phi = \sigma$

$$\langle T(h)\, \sigma(g_1, j_1)\rangle_{-+-}^{(\mathrm{cum})} = -\left(\frac{2}{j_1}\right)^{1/8} \frac{1}{(h+1)^4}\, \frac{1}{4} \times B(h;\, g_1,\, j_1). \tag{B9}$$

Here B is the square bracket in Eq. (B1) with z and z_1 expressed in terms of h and $g_1,\ j_1$ by replacing $z \to z(h)$ and $z_1 \to z_1(h_1 = g_1 + i j_1)$ via the Moebius mapping. In the following we consider the case with both T and ϕ located on the imaginary axis [24] in which $\langle T\, \phi\rangle_{-+-}^{(\mathrm{cum})}$ must be *real* by mirror symmetry.

Since $z_1 - \bar{z}_1 \to 4 i j_1/(1 + j_1^2)$ and $|z_1| \to 1$ in this case, the quantity P in (B2) becomes

$$P \to \frac{1}{2 i j_1 (1 - i j_1)^2} \times \left[1 + 30 j_1^2 + j_1^4 - 2 i j_1 \left(1 - j_1^2\right)\right] \tag{B10}$$

and since

$$\frac{1}{z - z_1} \to \frac{-j j_1 + i(j + j_1) + 1}{2 i (j - j_1)}, \quad \frac{1}{z - \bar{z}_1} \to \frac{j j_1 + i(j - j_1) + 1}{2 i (j + j_1)}, \quad z_1 + \bar{z}_1 \to -2\, \frac{1 - j_1^2}{1 + j_1^2}, \tag{B11}$$

one finds the explicit form

$$\langle \sigma(g_1 = 0,\, j_1)\, T(h = i j)\rangle_{-+-}^{(\mathrm{cum})} = \left(\frac{2}{j_1}\right)^{1/8} \frac{j_1^2}{4}\, \frac{j^2\left(j_1^2 + 15\right) - 15 j_1^2 - 1}{\left(j^2 - j_1^2\right)^2 \left(j^2 + 1\right)\left(j_1^2 + 1\right)}. \tag{B12}$$

For $j_1 = 1$ Eq. (B12) is consistent with Eq. (4.9).

Likewise one finds from (B3) and (B4) with

$$Q \to -i\left(j_2^2 + 1\right)^2 \left[\frac{1}{\left(j_2^2 - 1 + 2 i j_2\right)^2} + \frac{1}{16\, j_2^2}\right] \tag{B13}$$

that

$$\langle T(h = i j)\, \epsilon(g_2 = 0,\, j_2)\rangle_{-+-}^{(\mathrm{cum})} = j_2\, \frac{j^2\left(j_2^4 + 2 j_2^2 - 15\right) - 15 j_2^4 + 2 j_2^2 + 1}{\left(j^2 - j_2^2\right)^2 \left(j^2 + 1\right)\left(j_2^2 + 1\right)^2}. \tag{B14}$$

APPENDIX C: MAPPING AN EQUILATERAL TRIANGLE TO THE UPPER HALF PLANE

The conformal transformation [25]

$$h(Z) = 2 \times 3^{3/4} \frac{\mathrm{sn}(Z,k)\,\mathrm{dn}(Z,k)}{[1+\mathrm{cn}(Z,k)]^2}, \quad k = 2^{-3/2}(1+\sqrt{3}),$$
$$Z = \frac{Y_C}{y_C} \times z, \quad Y_C \equiv 2\mathbf{K}(k'), \quad k' \equiv \sqrt{1-k^2} = \frac{1}{2}(2-\sqrt{3})^{1/2} \tag{C1}$$

maps the interior of the equilateral triangle of side length $\mathscr{W}$ and height $y_C = (\sqrt{3}/2)\mathscr{W}$ in the $z = x + iy$ plane with corners at

$$z = z_A = -\mathscr{W}/2, \quad z_B = \mathscr{W}/2, \quad z_C = iy_C = i(\sqrt{3}/2)\mathscr{W} \tag{C2}$$

to the upper half h plane where the images of the corners are at

$$h = (h_A,\ h_B,\ h_C) = (-1,\ 1,\ \infty). \tag{C3}$$

The mapping of the corner z_C to $h = \infty$ arises from $\mathrm{cn}(2i\mathbf{K}(\sqrt{1-k^2}), k) = -1$, a relation that applies for arbitrary k. The particular value of k given in Eq. (C1) takes care that the images of the left and right boundary sides of the triangle are located on the real axis of the half plane. Due to the prefactor $2 \times 3^{3/4}$ they are given by the half lines $-\infty < h < -1$ and $1 < h < +\infty$, respectively, while the remaining interval $-1 < h < 1$ is the image of the triangle's base side. The inverse transformation mapping the upper half h plane to the triangle in the Z plane has the Schwarz-Christoffel form

$$Z(h) = 2 \times 3^{-3/4} \int_0^h dh'\,(1-h'^2)^{-2/3} \tag{C4}$$

with a prefactor that follows from comparing (C4) and (C1) for $h \to 0$ and $Z \to 0$, respectively.

Note the rescaling factor

$$S(Z) \equiv dh/dZ = -2 \times 3^{3/4} \times \frac{2k^2\mathrm{sn}^2 + \mathrm{cn} - 2}{(1+\mathrm{cn})^2}$$
$$= (dZ/dh)^{-1} = \frac{1}{2}3^{3/4}[1-h^2(Z)]^{2/3}, \quad Z = X + iY \tag{C5}$$

of the transformation (C1). Here the argument of sn and cn is (Z, k).

In the following we concentrate on the vertical midline of the triangle corresponding to $Z = i \times Y$, which is mapped to the vertical midline $h = i \times j$ in the upper half h plane via

$$j(Y) = 2 \times 3^{3/4} \times \frac{\mathrm{sn}(Y,k')\,\mathrm{dn}(Y,k')}{[1+\mathrm{cn}(Y,k')]^2} \tag{C6}$$

with the inverse transformation

$$Y(j) = 2 \times 3^{-3/4} \int_0^j dj'\,(1+j'^2)^{-2/3} \tag{C7}$$

that follow from Eqs. (C1) and (C4), respectively [26]. We note the values

$$Y(j=\infty) \equiv Y_C \equiv 2\mathbf{K}(k') = 3.196284004, \quad Y(j=1) \equiv Y_0 = 0.7432642107 \tag{C8}$$

and their ratio $Y_0/Y_C = y_0/y_C = 0.2325401027$. Here $Z_0 = iY_0$ is the position on the midline where $\langle\sigma\rangle_{\mathrm{triangle}}$ in (5.3) vanishes since it is mapped to $h = i$ where $j = 1$.

The corresponding rescaling factor reads

$$S(iY) = 2 \times 3^{3/4} \times \frac{2k'^2\,\mathrm{cn}^2 - \mathrm{cn} + 2(1-k'^2)}{(1+\mathrm{cn})^2} = \frac{1}{2}\,3^{3/4}\,[1+j^2(Y)]^{2/3}, \tag{C9}$$

where the argument of cn is given by (Y, k'). This follows from Eq. (C5).

For j close to 1, i.e., Y close to Y_0, Eqs. (C7) and (C9) imply up to first order

$$j(Y) - 1 \to S_0\,(Y - Y_0), \quad S(iY) \to S_0\left[1 + \tfrac{2}{3}S_0\,(Y - Y_0)\right], \tag{C10}$$

where

$$S_0 \equiv S(iY_0) = 2^{(2/3)-1}\,3^{3/4}. \tag{C11}$$

Near the base line and near the upper corner $Y \to Y_C - \delta$, Eqs. (C6) and (C9) yield

$$j(Y) \to 3^{3/4}\,\frac{Y}{2}, \quad S(iY) \to 3^{3/4}\,\frac{1}{2} \tag{C12}$$

and

$$j(Y) \to 3^{3/4}\,(\delta/2)^{-3}, \quad S(iY) \to 3^{3/4}\,\tfrac{1}{2} \times j(Y)^{4/3} \equiv 3^{3/4}\,\tfrac{3}{2}\,(\delta/2)^{-4}, \tag{C13}$$

respectively. Written in terms of the height y_C of the triangle, Eq. (C1) yields

$$Y = \frac{y}{y_C}\,Y_C, \quad \delta = \frac{y_C - y}{y_C}\,Y_C\,. \tag{C14}$$

APPENDIX D: ORDER PARAMETER PROFILE IN THE SQUARE

Here we evaluate the order-parameter profile in the $\mathscr{W} \times \mathscr{W}$ square addressed in Sec. VI which we need to calculate via the OPE (A1) the corresponding two-point function $\langle \sigma\, \epsilon \rangle_{SQ}$ near the center. The profile follows by conformal transformations like in Eqs. (B7)–(B13) in Ref. [6] from that in the upper half $H = G + iJ$ plane. For the present boundary conditions in the square the real axis $J = 0$ is to be endowed with boundary conditions $-+-+-$ for

$$-\infty < G < -C, \quad -C < G < -c, \quad -c < G < c, \quad c < G < C, \quad C < G < +\infty, \tag{D1}$$

respectively, where

$$C = \sqrt{2} + 1, \quad c = \sqrt{2} - 1. \tag{D2}$$

For completeness we note the expression

$$\langle \sigma(H, \bar{H}) \rangle = -\left(\frac{4i}{H - \bar{H}}\right)^{1/8} \frac{1}{C^4 + 14C^2c^2 + c^4} \times \frac{1}{|H^4 - (C^2 + c^2)H^2 + C^2c^2|} \times \{8C^2c^2[2(H\bar{H})^2 - (C^2 + c^2)(H^2 + \bar{H}^2) + 2C^2c^2] + (C^2 - c^2)^2[(H\bar{H})^2 - (C^2 + c^2)H\bar{H} + C^2c^2]\} \tag{D3}$$

that applies to *arbitrary* $0 < c < C$, which is of interest for calculating the order parameter profile inside a rectangle of arbitrary aspect ratio. One easily checks that, on approaching the boundary $H = G$, the RHS of (D3) turns to the expected behavior $-(2/J)^{1/8}\,\mathrm{sgn}(G^2 - C^2)\,\mathrm{sgn}(G^2 - c^2)$. Equation (D3) follows from Eqs. (17) and (18a) in Ref. [4]. For the special values in (D2) it follows that $C^2c^2 = 1,\ C^2 + c^2 = 6,\ (C^2 - c^2)^2 = 32,\ C^4 + c^4 = 34$, and $C^4 + 14C^2c^2 + c^4 = 48$ and (D3) becomes

$$\langle \sigma(H, \bar{H}) \rangle = -\left(\frac{4i}{H - \bar{H}}\right)^{1/8} \frac{(H\bar{H})^2 - H^2 - \bar{H}^2 - 4H\bar{H} + 1}{|H^4 - 6H^2 + 1|}. \tag{D4}$$

The RHS of Eq. (D4) vanishes for $H = i$ which is the preimage of the center of the square. The Möbius transformation

$$H(w) = i\,\frac{1 + w}{1 - w}, \quad \frac{dH}{dw} = \frac{2i}{(1 - w)^2} \tag{D5}$$

relates the upper half H plane to the interior of the unit circle in the $w = u + iv$ plane. Since $H(w \equiv \exp(i\alpha)) = -\cot(\alpha/2)$, the points $\exp(i\alpha)$ on the periphery of the circle with α values $\pi/4,\ 3\pi/4,\ 5\pi/4,\ 7\pi/4$ map to the switch points $-C,\ -c,\ c,\ C$ on the real axis $H = G$ in Eq. (D1) with (D2) taken into account. Moreover, for values $0,\ \pi/2, \pi, 3\pi/2$ the points map to $-\infty,\ -1,\ 0,\ 1$, respectively. The center $w = 0$ of the circle maps to $H = i$. Finally the Schwarz-Christoffel transformation

$$z(w) = \Lambda \int_0^w \frac{d\omega}{\sqrt{1 + \omega^4}} \tag{D6}$$

maps the interior of the circle to the interior of our $\mathscr{W} \times \mathscr{W}$ square in the z plane. Here Λ is from below (6.5). Since the above-mentioned points with $\pi/4,\ 3\pi/4,\ 5\pi/4,\ 7\pi/4$ on the boundary of the circle are mapped [27] to the corners $z = (\mathscr{W}/2)\,[1 + i,\ -1 + i,\ -1 - i,\ 1 - i]$ and those with $0,\ \pi/2, \pi, 3\pi/2$ to the side midpoints $z = (\mathscr{W}/2)\,[1,\ i,\ -1,\ -i]$ of the square, it has the desired boundary conditions.

To derive the one-point function in (6.6) we must understand only the prefactor since the dependence on x_1, y_1 is dictated by the symmetries (6.1), (6.2). It is thus sufficient to calculate the form of (6.6) along the x direction, which in the H plane corresponds to the imaginary axis $H = iJ$. The corresponding dependence in the circle along the u direction follows from (D4), (D5) and reads

$$\langle \sigma(u, u) \rangle = -\left(\frac{4}{1 - u^2}\right)^{1/8} \frac{2u^2}{1 + u^4}. \tag{D7}$$

Since $dw/dz = \sqrt{1 + w^4}/\Lambda$ one finds for $|x| \ll \mathscr{W}$ where $u \ll 1$ the near center behavior

$$\langle \sigma(x, x) \rangle_{SQ} \to -\Lambda^{-1/8}\,4^{1/8}\,2u^2 \to -\left(\frac{4}{\Lambda}\right)^{1/8} 2\left(\frac{x}{\Lambda}\right)^2 \tag{D8}$$

along the x direction and, due to symmetry, one finds the result (6.6). This allows us to evaluate in Appendix A 7 the behavior of the response function near the center of the square.

[1] H. W. Diehl, in *Phase Transitions and Critical Phenomena,* edited by C. Domb and J. L. Lebowitz (Academic, London, 1986), Vol. 10, p. 76; H. W. Diehl, Int. J. Mod. Phys. B **11**, 3503 (1997).

[2] J. L. Cardy, Nucl. Phys. B **240**, 514 (1984).

[3] T. W. Burkhardt and T. Xue, Nucl. Phys. B **354**, 653 (1991); Our notation *ab* for the mixed boundary means *ba* in the notation of this reference.

[4] T. W. Burkhardt and I. Guim, Phys. Rev. B **47**, 14306 (1993).

[5] T. W. Burkhardt and E. Eisenriegler, Phys. Rev. E **103**, 012120 (2021).

[6] E. Eisenriegler, Phys. Rev. E **108**, 044133 (2023).

[7] A. A. Belavin, A. M. Polyakov, and A. B. Zamolodchikov, Nucl. Phys. B **241**, 333 (1984).

[8] Microscopically we have an Ising lattice model in mind with a ferromagnetic interaction between nearest neighbors.

[9] For relating $\epsilon(\mathbf{r})$ to the products of nearest neighbor spins see, e.g., Eq. (D2) in Ref. [6].

[10] The corresponding correlation between spins a short *mesoscopic* distance $|\mathbf{r}_{12}|$ apart is related to $\langle\epsilon\rangle$ via $\langle\sigma\times\sigma\rangle - \langle\sigma\times\sigma\rangle_{\rm bulk} \to -(1/2)\,|\mathbf{r}_{12}|^{1-(1/4)}\,\langle\epsilon\rangle$. This quantitative universal relationship follows on including the next-to-leading term in the OPE (1.1) of $\sigma\times\sigma$; see, e.g., Eq. (2.14) in Ref. [5].

[11] Equations (1.3) are derived from comparing with the exact expression

$$\langle\sigma(\mathbf{r}_1)\epsilon(\mathbf{r}_2)\sigma(\mathbf{r}_3)\rangle_{\rm bulk} = -|\mathbf{r}_{13}|^{3/4}/(2\,|\mathbf{r}_{12}||\mathbf{r}_{23}|)$$

of the bulk three point function when expanded about $\mathbf{r}_1$ and $\mathbf{r}_2$ in the limit $|\mathbf{r}_{12}| \ll |\mathbf{r}_{31}|, |\mathbf{r}_{32}|$. Higher order terms of the BOE are given in Appendix A.

[12] Like the operator product $\sigma\times\epsilon$ on the left hand side of the OPE (1.3) its right hand side must change sign on reversing all Ising spins and is composed of σ and its descendents. Unlike the OPEs in (1.1) there is no operator-free term in (1.3).

[13] The second term in the cumulant (1.2) is regular for $|\mathbf{r}_{12}| \to 0$ and does not contribute to the singular behavior of the terms given by the BOE (1.3).

[14] While y_0 denotes in Secs. I–III a given distance from the real axis of arbitrary value, in Sec. V it denotes the value of y on the midline of the triangle where $\langle\sigma\rangle_{\rm triangle}$ vanishes.

[15] At first sight the "disorder *enhancing* the order" effect discussed in paragraph (iii) in the Introduction might look surprising. A qualitative understanding in the framework of a square lattice model has been given by T. W. Burkhardt. Choosing to effect the increase of the energy density at $(x_2 = 0, y_2 = y_0)$ by adding a horizontal *antiferromagnetic* bond between Ising spins $S(-1, y_0)$ and $S(1, y_0)$, due to the $+-$ boundary condition the preferred configuration of the additional bond will be $S(-1, y_0)$ = up and $S(1, y_0)$ = down. On the neighboring spins $S(-2, y_0)$, $S(2, y_0)$, etc., this bond configuration acts in the same way as the boundary condition and enhances the order. An additional vertical bond between $S(0, y_0 - 1)$ and $S(0, y_0 + 1)$, needed for the proper lattice symmetry of ϵ, does not change the enhancement effect.

[16] For the primary operators $\phi = \sigma$ or $\phi = \epsilon$ approaching a boundary section on the x axis with boundary condition $a = +$ or $-$ the "boundary operator expansion" BOE has the form

$$\phi(x, y) - \langle\phi\rangle_a \to \mu_a^{(\phi)}\, y^{2-x_\phi} T(x), \quad y \to 0.$$

Here the leading boundary operator T is the stress tensor, $x_\phi = 1/8$ or 1 are the scaling dimensions of σ or ϵ, and

$$\mu_+^{(\sigma)} = -\mu_-^{(\sigma)} = -2^{1/8}\ \mu_+^{(\epsilon)} = \mu_-^{(\epsilon)} = 4.$$

For details see Eqs. (3.1)–(3.5) in Ref. [5].

[17] In order to facilitate the conformal transformations to other geometries, the exact results of Ref. [3] are written in complex notation.

[18] Consider the cumulant $\langle\phi\Phi\rangle_{\rm G}^{\rm (cum)}$ between two primary operators ϕ and Φ embedded in a geometry G with a corner, such as the triangle discussed in Sec. V. When ϕ approaches the tip of the corner and Φ is at a fixed finite distance from it, the cumulant takes the form $F \times \langle\mathcal{T}\,\Phi\rangle_{\rm G}^{\rm (cum)}$, where $\mathcal{T}$ is a "corner operator" which is located right at the tip of the corner and F depends on the "small distance" d of ϕ from the corner. If the two sides of the corner belong to the same universality class the distance dependence is $F \propto d^{(2\pi/\gamma)-x_\phi}$, where γ is the angle enclosed by the corner; cf. Eq. (4.5) in Ref. [6]. In case of ϵ and σ approaching the corner at point C of the equilateral triangle with $\gamma = \pi/3$ one finds $F \propto d^5$ and $d^{6-(1/8)}$, respectively, since $x_\phi = x_\epsilon = 1$ and $x_\sigma = 1/8$. Approaching a straight-line boundary such as the base side of the triangle can be viewed as approaching a corner with $\gamma = \pi$, which for $x_\phi = 1$ or 1/8 yields the BOE dependencies d^1 or $d^{2-(1/8)}$. Equations (5.10)ff and panels (a) and (b) in Fig. 3 for the triangle are in agreement with these dependencies.

[19] The small value $y_0 = 0.2325 \times y_{\rm C}$ of the zero of $\langle\sigma\rangle_{\rm triangle}$ on the midline is not surprising. Only the base line has boundary condition $+$, while the other two sides of the triangle both have $-$. So y_0 is definitely smaller than the value $y = y_{\rm center} = y_{\rm C}/3$ of the triangle's center where $\langle\sigma\rangle_{\rm triangle}$ obviously is negative. Note that the image in the $-+-$ half plane of $iy_{\rm center}$ is $h_{\rm center} = i\sqrt{3}$.

[20] Once in a given geometry $\mathcal{G}$ the average $\langle T(z)\,\sigma(z_1,\,\bar z_1)\rangle_{\mathcal{G}}$ is known, the form of the corresponding average $\langle L_{-p}\,\sigma(z_1,\,\bar z_1)\rangle_{\mathcal{G}}$ follows most easily from averaging the inverse relation

$$T(z)\,\sigma(z_1,\,\bar z_1) = \sum_{k=-\infty}^{\infty} (z - z_1)^{k-2}\,(L_{-k}\,\sigma(z_1,\,\bar z_1)).$$

[21] M. P. Mattis, Nucl. Phys. B **285**, 671 (1987).

[22] Equation (B2) in A. Squarcini, A. Maciolek, E. Eisenriegler, and S. Dietrich, JSTAT/2020/043208, contains a misprint. Instead of $2\Theta{\rm Re}(\mathcal{T})$ its right hand side should read $-2\Theta\,{\rm Re}(\mathcal{T})$.

[23] For the $\mathscr{a}$ term one needs $\langle L_{-1}\sigma\rangle_{-+-}$ for which Eq. (A26) yields $\partial_{h_1}\langle\sigma\rangle_{-+-} = 2^{(1/8)-1} \times i$.

[24] For $h = ij$ the Moebius transformation (4.2) reduces to $z = (j^2 - 1 + 2ij)/(j^2 + 1)$ so that z varies from -1 to 1 along the upper unit circle of the $+-$ plane as j varies from 0 to ∞.

[25] Compare with Sec. 13.8 in H. Kober, Dictionary of Conformal Representations, Dover Publications 1957. The quantity $w_2 \equiv (4\pi^2/3)(\Gamma(2/3))^{-3}$ there is in terms of our $Z_{\rm B}$ in (C2) given by $2^{-2/3}3^{3/4} \times 2Z_{\rm B}$, (Dover Publications, 1957).

[26] Consistency between the upper limits $Y = 2\mathbf{K}(k')$ and $j = \infty$ in Eqs. (C6) and (C7) is guaranteed by the relation $\mathbf{K}(k') = (3^{-1/2}\pi)^{3/2}/[\Gamma(5/6)\Gamma(2/3)]$.

[27] For the mapping (D6) note that $\int_0^1 d\omega\,[(1+\omega^4)^{-1/2},\,(1-\omega^4)^{-1/2}] = [1/2,\,1/\sqrt{2}]\,\mathbf{K}(1/\sqrt{2})$.